

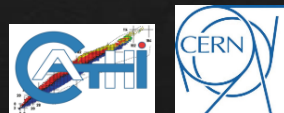
SRF Developments at the HIE ISOLDE Accelerating Structures Working Group

W. Venturini Delsolaro
on behalf of the ASWG:

L. Alberty, K. Artoos, S. Calatroni, O. Capatina, A. D'Elia,
M. Elias, **N. M. Jecklin**, M. A. Fraser, Y. Kadi, P. Maesen,
I. Mondino, E. Montesinos, A. Myazaki, G. Rosaz, K. Schirm,
A. R. M. Sublet, M. Therasse, R. Valera, D. Valuch, **P. Zhang**



CATHI final review meeting
Barcelona, Spain, 22-26 September 2014



Contents

- ASWG mandate
- HIE ISOLDE cavity technical aspects:
 - QWR specifications
 - Cavity technologies
 - Development of Nb/Cu QWR for HIE ISOLDE
 - Coupling system
 - Tuning system
 - LLRF
- Conclusions

HIE-ISOLDE ASWG: facts and figures

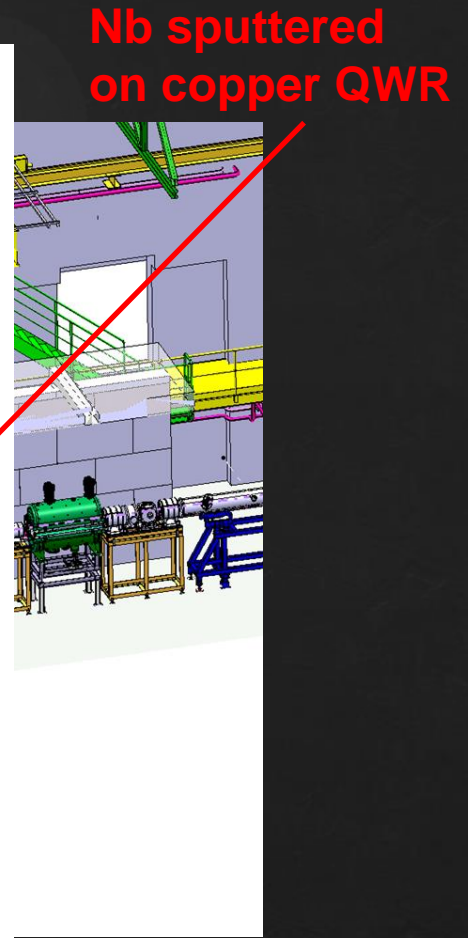
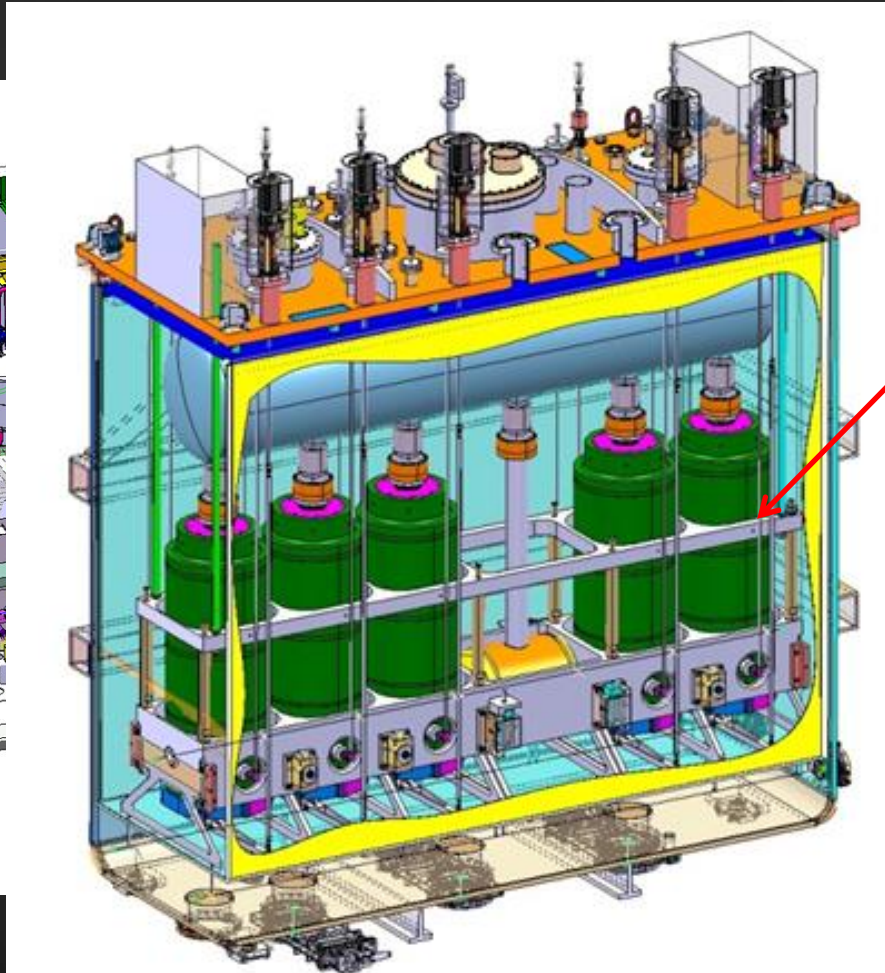
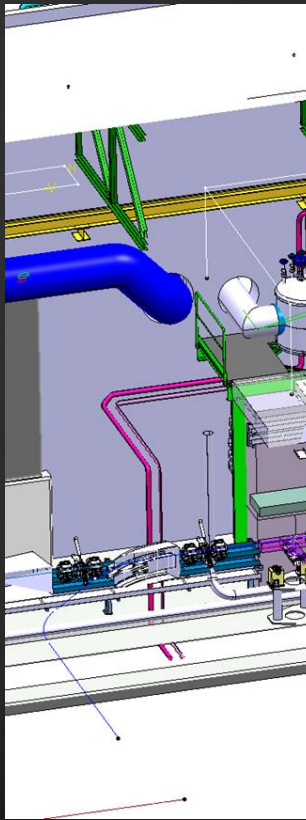
- Design, technological choices and production
 - HIE ISOLDE Accelerating Cavities
 - Fundamental Coupler
 - Tuning System
- Multidisciplinary team: material science, RF and mechanical engineering, and more.
- **CATHI fellows first actors**
- Regular (now weekly) meetings
- Minutes and slides on EDMS

The image shows two side-by-side screenshots from the EDMS (Engineering Data Management System) interface. The left screenshot displays a hierarchical tree view of the HIE-ISOLDE project structure, with the 'RF ACCELERATING STRUCTURES' folder expanded to show 'Technical Coordination Meetings'. The right screenshot shows the 'EDMS Project Page' for 'CERN-000083267 v.0', specifically for 'Technical Coordination Meetings'. It features a search bar, a status indicator 'In Work', and a list of documents. The document list includes entries for meetings from May 2014 to July 2014, each with associated documents like 'Annex1', 'Annex2', and 'Minutes' in various formats (pptx, docx, pdf, jpg, png).

Document ID	Version	Meeting Title	Date	Status
HIE-ACSTN-MIN-0022	v.1	HIE-ISOLDE Accelerating Structures WG meeting	21 May 2014	Released
HIE-ACSTN-MIN-0023	v.1	HIE-ISOLDE Accelerating Structures WG meeting	28 May 2014	Released
HIE-ACSTN-MIN-0024	v.1	HIE-ISOLDE Accelerating Structures WG meeting	4 June 2014	Released
HIE-ACSTN-MIN-0025	v.1	HIE-ISOLDE Accelerating Structures WG meeting	11 June 2014	Released
HIE-ACSTN-MIN-0026	v.1	HIE-ISOLDE Accelerating Structures WG meeting	18 June 2014	Released
HIE-ACSTN-MIN-0027	v.1	HIE-ISOLDE Accelerating Structures WG meeting	25 June 2014	Released
HIE-ACSTN-MIN-0028	v.1	HIE-ISOLDE Accelerating Structures WG meeting	2 July 2014	Released
HIE-ACSTN-MIN-0029	v.1	HIE-ISOLDE Accelerating Structures WG meeting	9 July 2014	Released
HIE-ACSTN-MIN-0030	v.1	HIE-ISOLDE Accelerating Structures WG meeting	16 July 2014	Released

The HIE ISOLDE Cryomodules

Common vacuum concept - Actively cooled thermal shield-
Superconducting active elements: RF cavities and solenoid



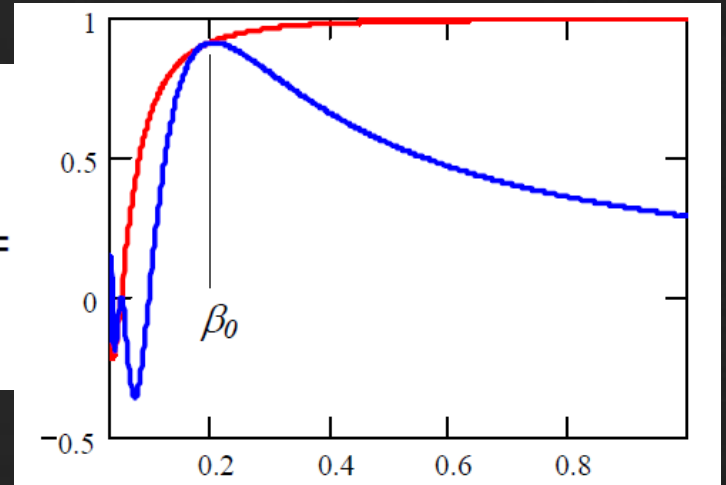
**Nb sputtered
on copper QWR**

Why quarter wave resonators

At low particle velocities, effective acceleration depends on transit time

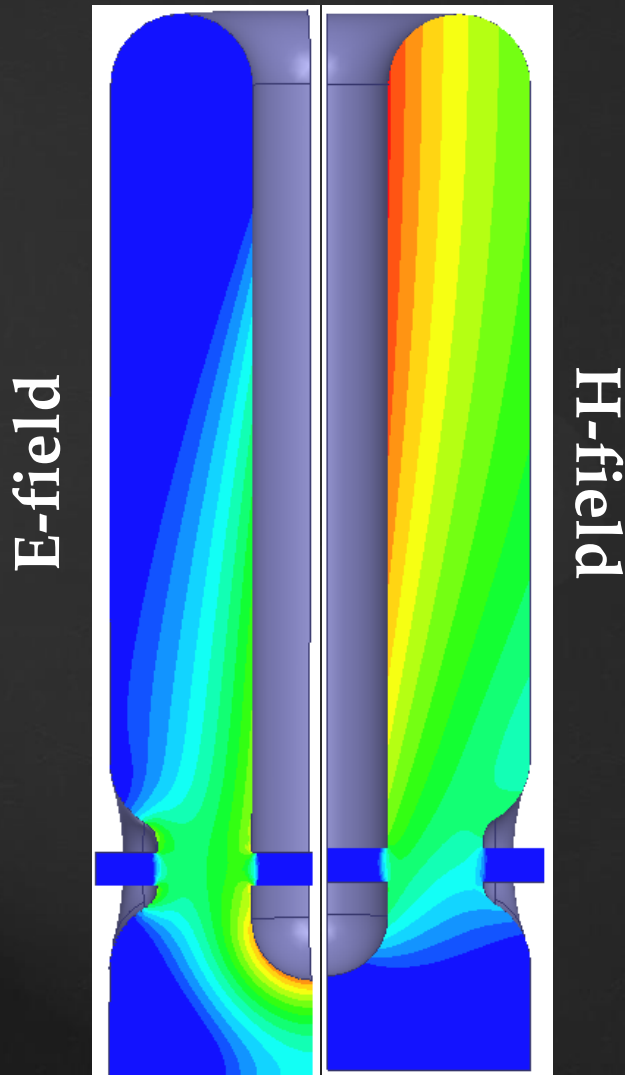
$$\Delta W_p = qE_a LT(\beta) \cos \varphi$$

$$T(\beta) =$$



- Low frequency improves the TTF
- Multi (two) gap structure \rightarrow TTF curve with a maximum (optimum beta)
- Quarter wave resonators have broader $TTF(\beta)$ curves (larger energy acceptance); relatively favourable field ratios for a low beta structure, and high frequency of the lowest mechanical mode
- Low frequency \rightarrow low BCS surface resistance \rightarrow 4.2 K operation

High beta QWR design (electromagnetic)



HIE ISOLDE	Baseline [†]	New*
f_0 at 4.5 K [MHz]	101.28	101.28
β_{opt} [%]	10.86	10.88
TTF at β_{opt}	0.9	0.9
R/Q [Ω] (incl. TTF)	554	556
E_p/E_{acc}	5.5	5.0
H_p/E_{acc} [G/(MV/m)]	95.4	95.3
U/E_{acc}^2 [mJ]/(MV/m) ²	208	207
$G=R_s Q$ [Ω]	30.7	30.8
P_{diss} @ 6 MV/m [W]	10	10
P_{diss} on bottom plate [W]	0.0035	0.0018

[†]Original tuning plate *Simplified tuning plate

Choice of cavity technology

Superconducting option

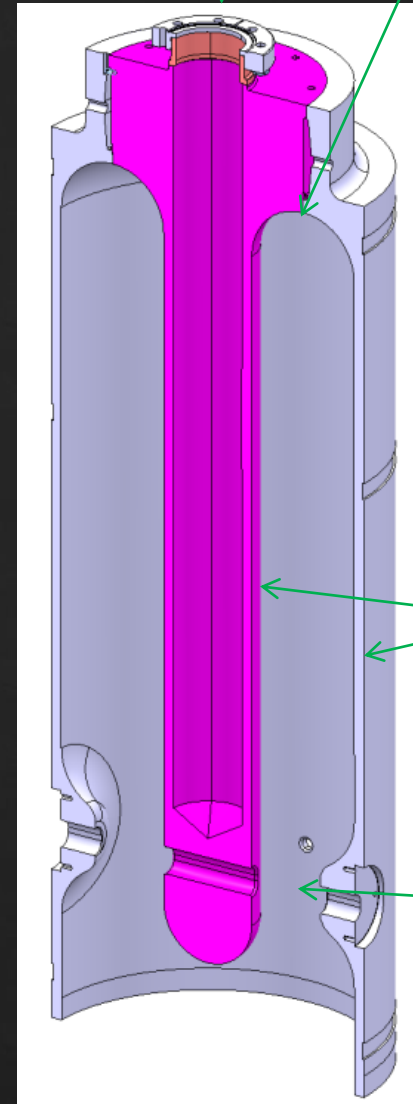
- High Q (low power dissipation)
- Cryogenics
- High CW fields (30 MV/m peak)
- Possible field emission, X rays

Niobium sputtering on copper

- Thermal stability
- Mechanical stability → less sensitive to He pressure fluctuations and to mechanical vibrations → Low RF power
- Less sensitive to magnetic fields → no need of shielding the cryostat
- Potentially cheaper (especially for large series)
- Possible to recycle substrates

Liquid Helium space

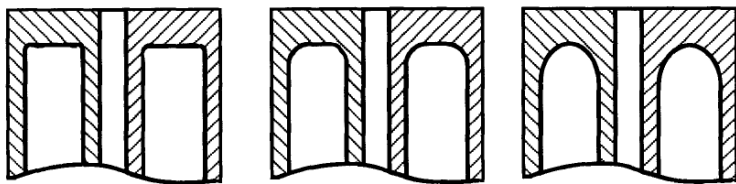
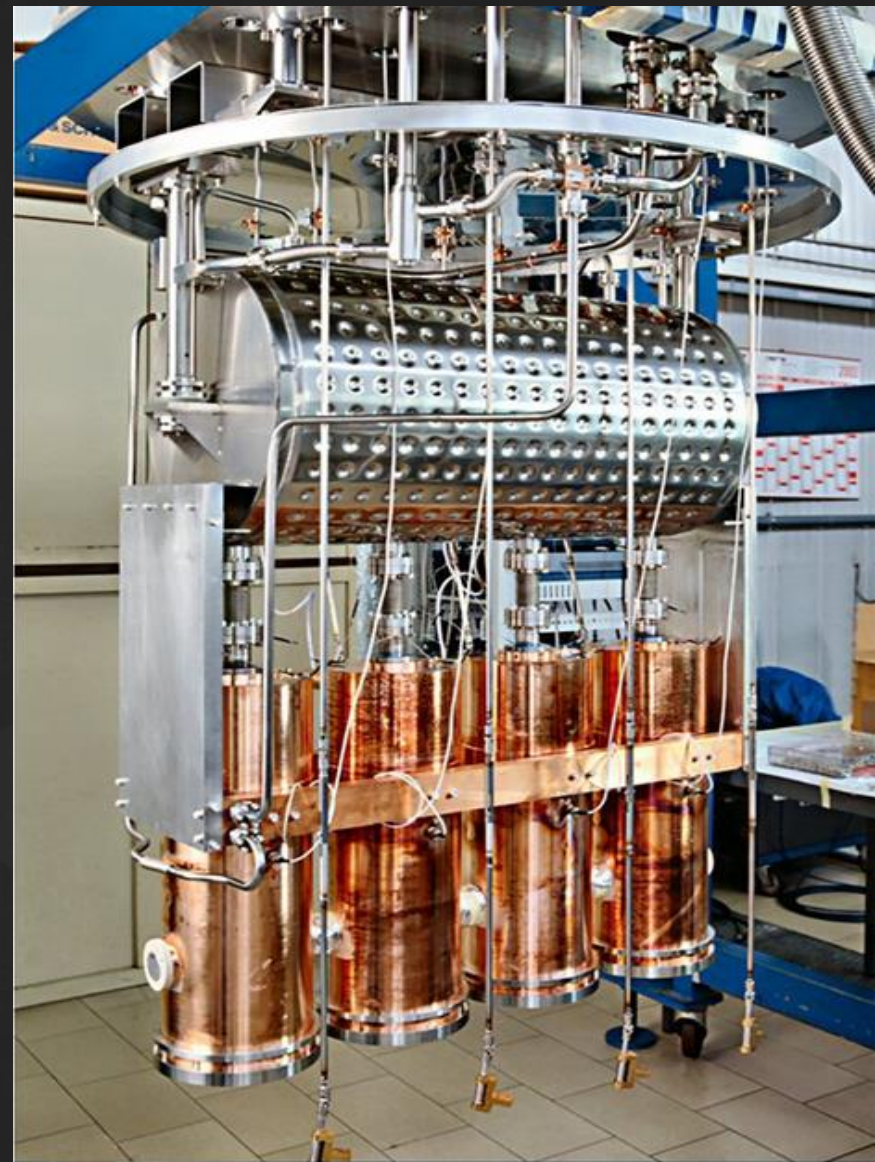
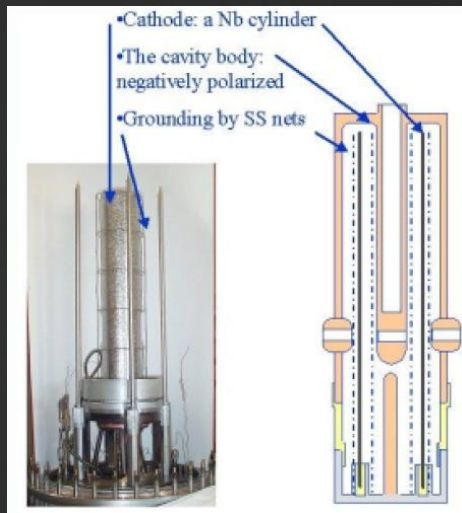
E-beam weld



OFE
copper
walls

Beam axis

The ALPI experience: over 50 Nb/Cu QWR made at INFN -LNL installed between 1999 and 2003



a

b

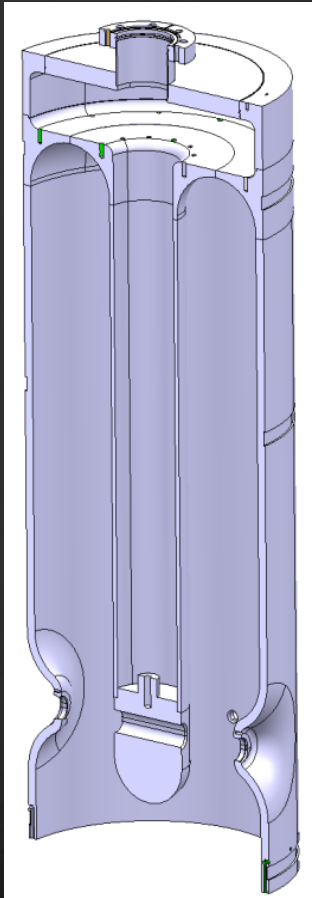
c

Fig. 6. Detail of resonator geometry: a) old model with curvature radius of 10 mm; b) modified model with curvature radius of 20 mm; c) definitive model with curvature radius of 30 mm.

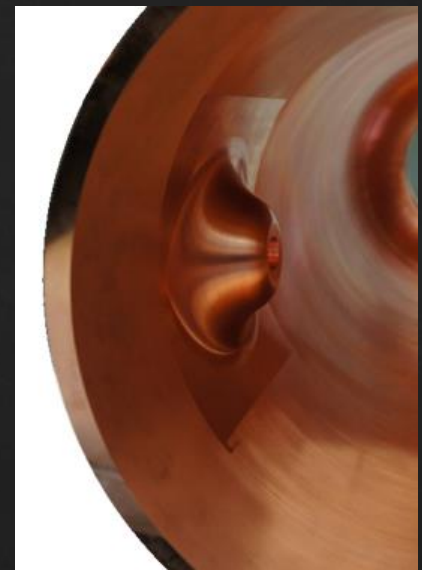
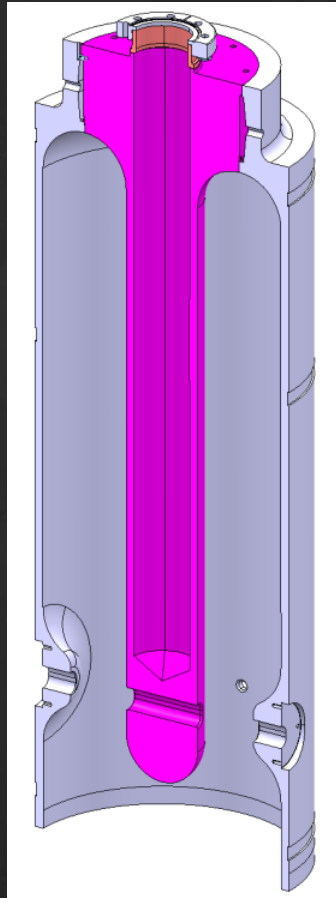
Evolution of resonator geometry
(from V. Palmieri, V. L. Ruzinov, S. Stark, et al;
*Proceedings of the 6th Workshop on RF
superconductivity, 1993*)

High beta QWR design (mechanical)

Version 1

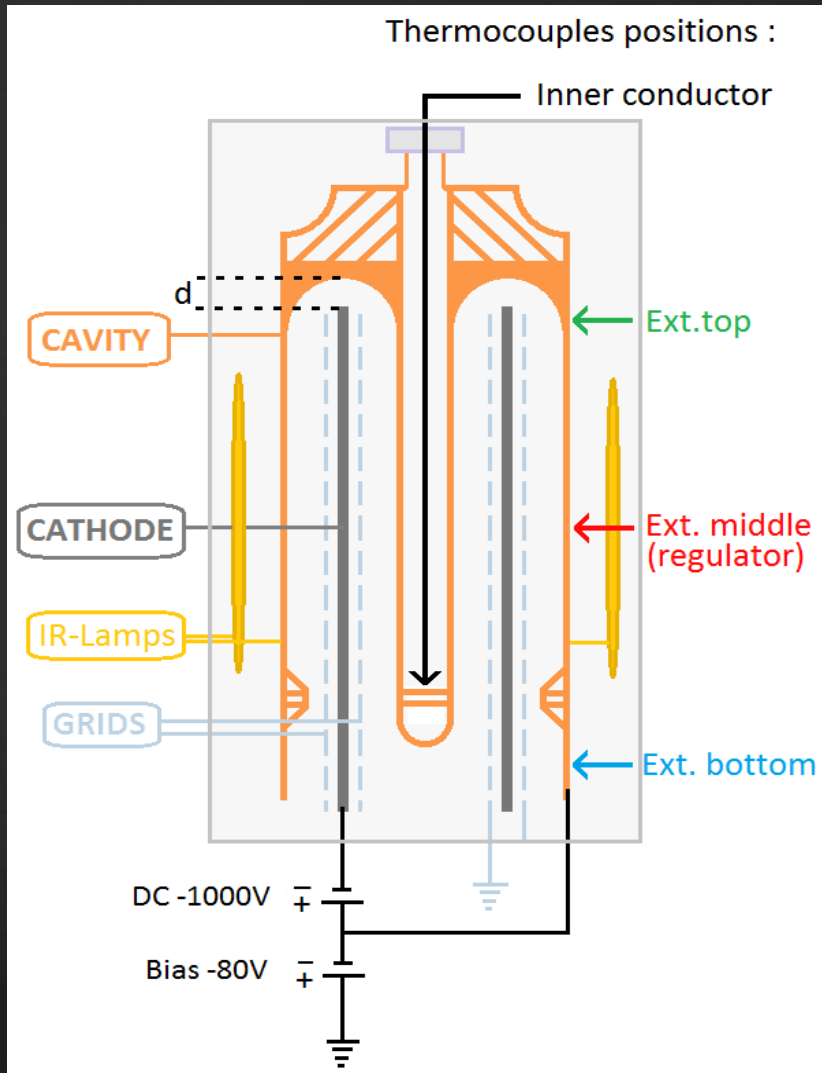


Version 2

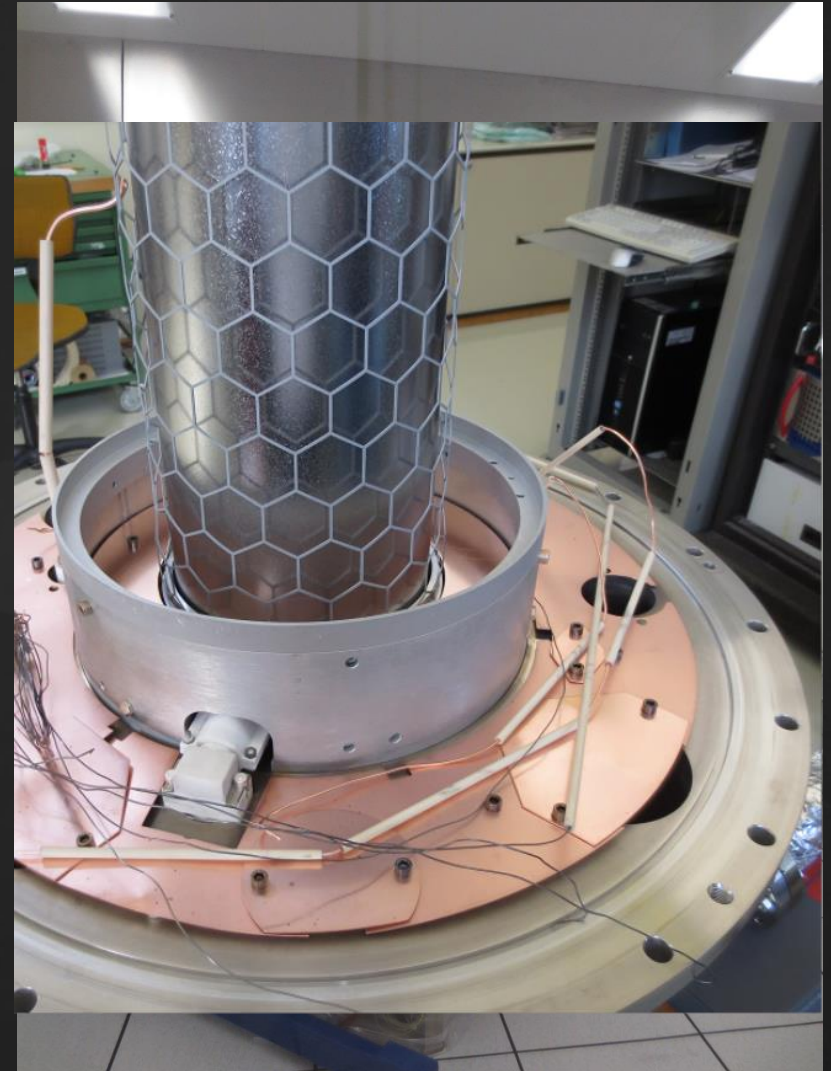


Bias diode sputtering system

Schematics



System assembly in ISO 5 clean room



Power dissipation, surface resistance

$$P_c = \frac{1}{2} R_s \int H^2 ds \quad Q_0 = \frac{\omega U}{P_c} = \frac{\Gamma}{R_s}$$

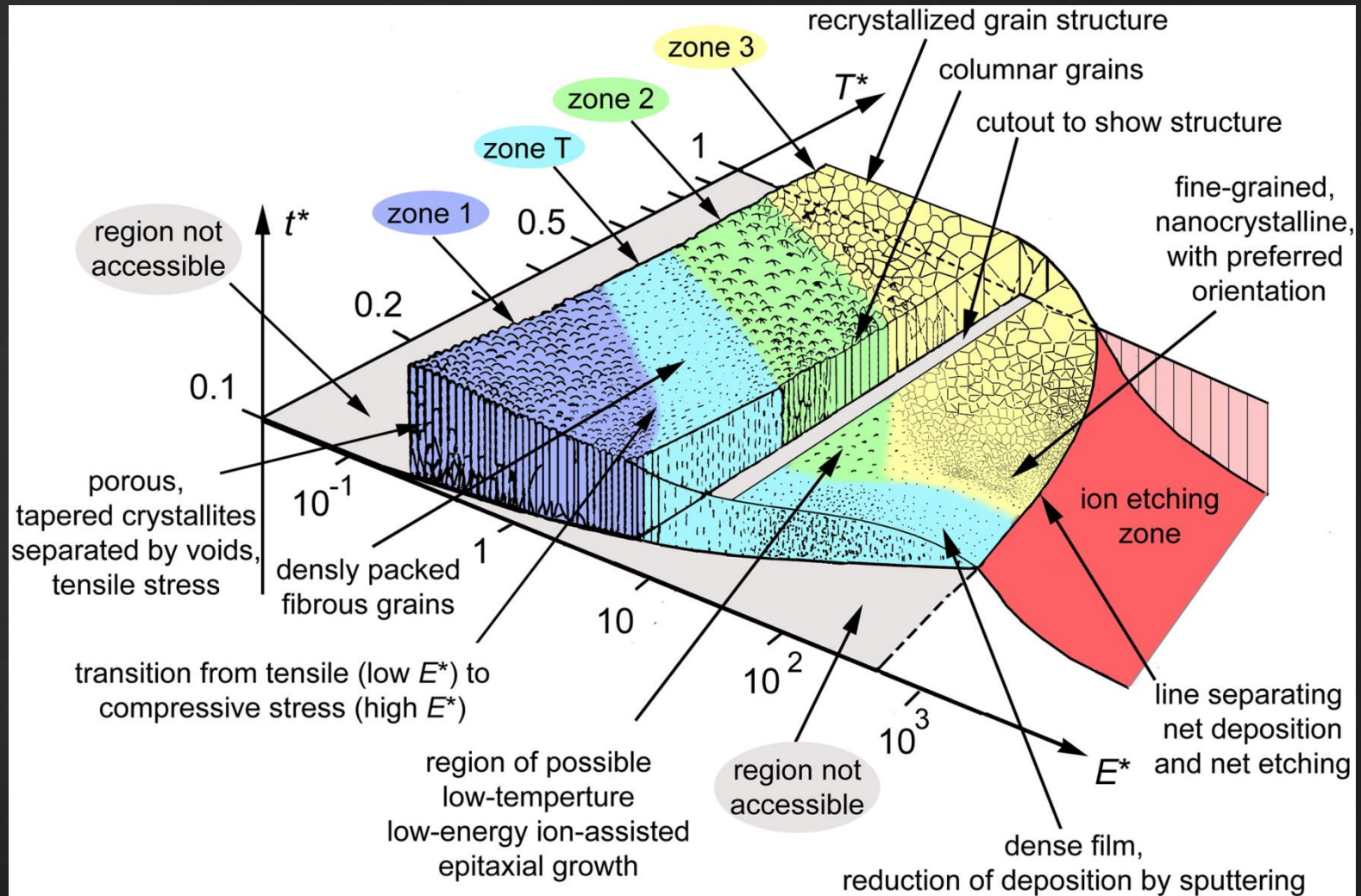
$$R_s = R_{BCS} + R_{res} \quad R_{BCS} = \frac{A\omega^2}{T} \exp\left(-\frac{\Delta}{k_B T}\right)$$

HIE ISOLDE low beta cavity:

R_{BCS} at 4.2 K and 101.28 MHz < 10% of total R_s

R_{res} is related to the "real" surface: defects, oxides, etc.

Thin film growth: structure zone models



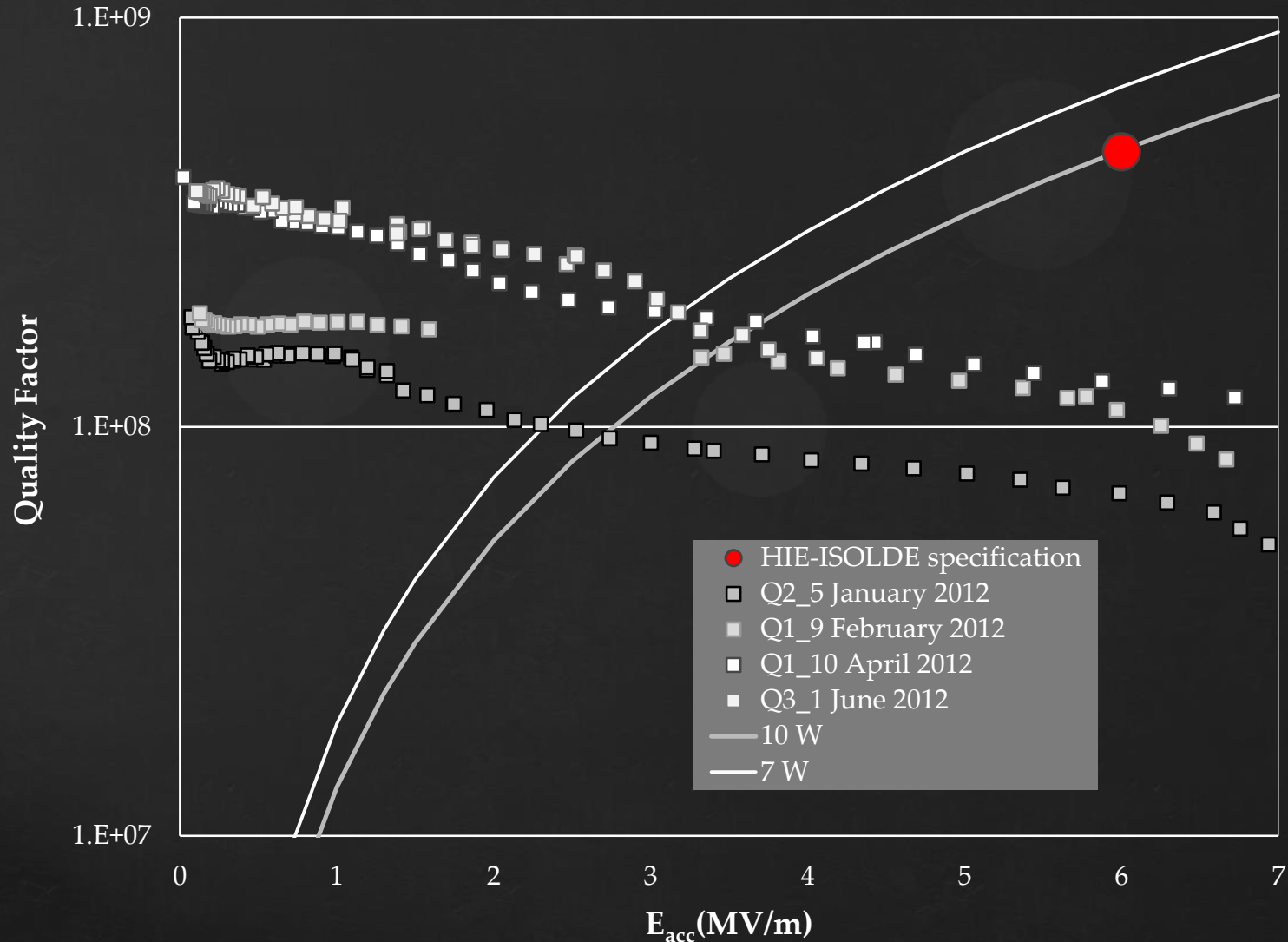
Roadmap of developments (2011-2013)

Strong development program focused on bias diode sputtering method. Main steps:

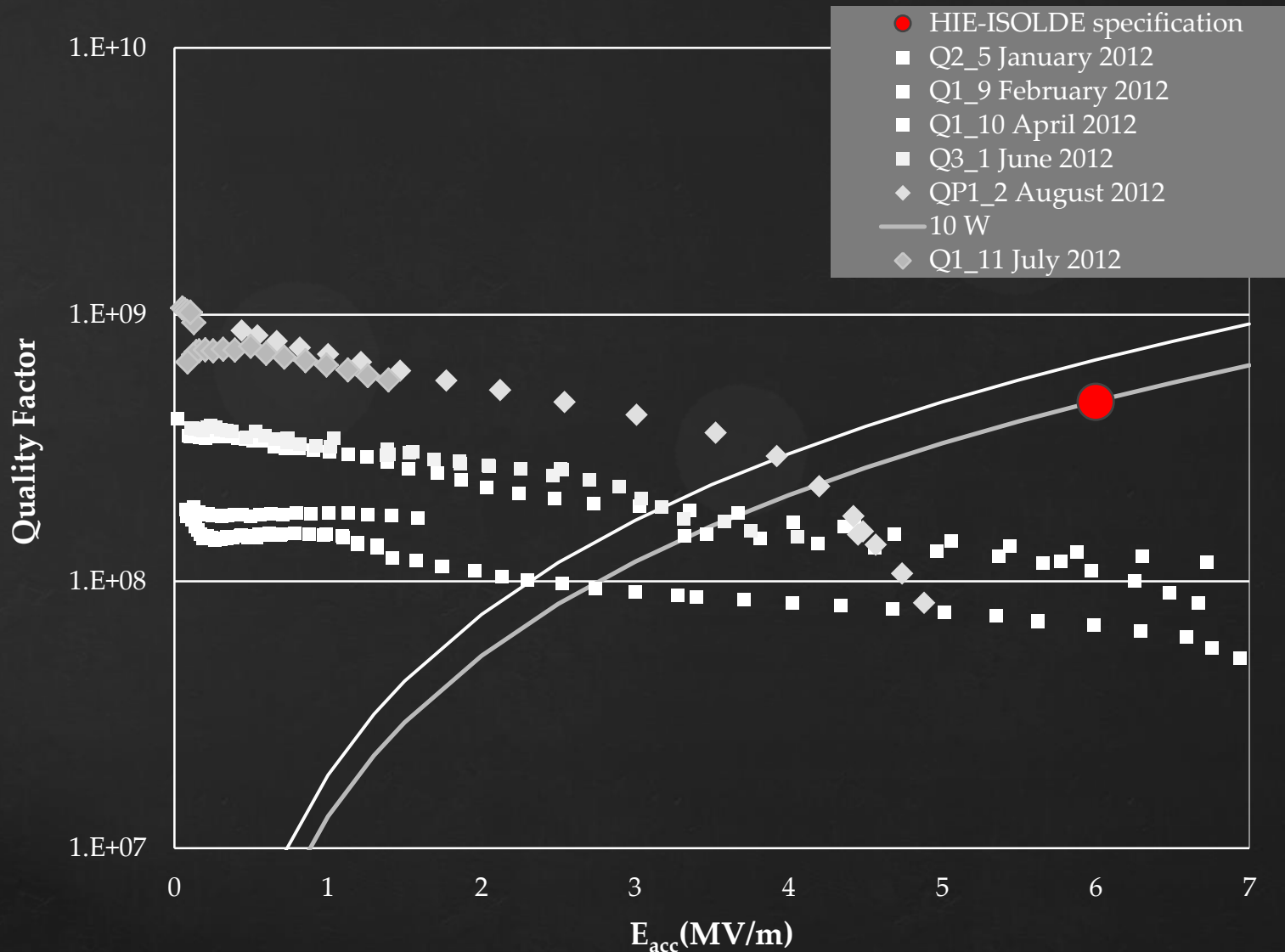
- Increasing baking and coating temperatures
- Increasing sputtering power (global deposition rate)
- Coating in steps
- Sputtering gas, venting gas
- Global film thickness
- Local film thickness

Increasing coating temperature,

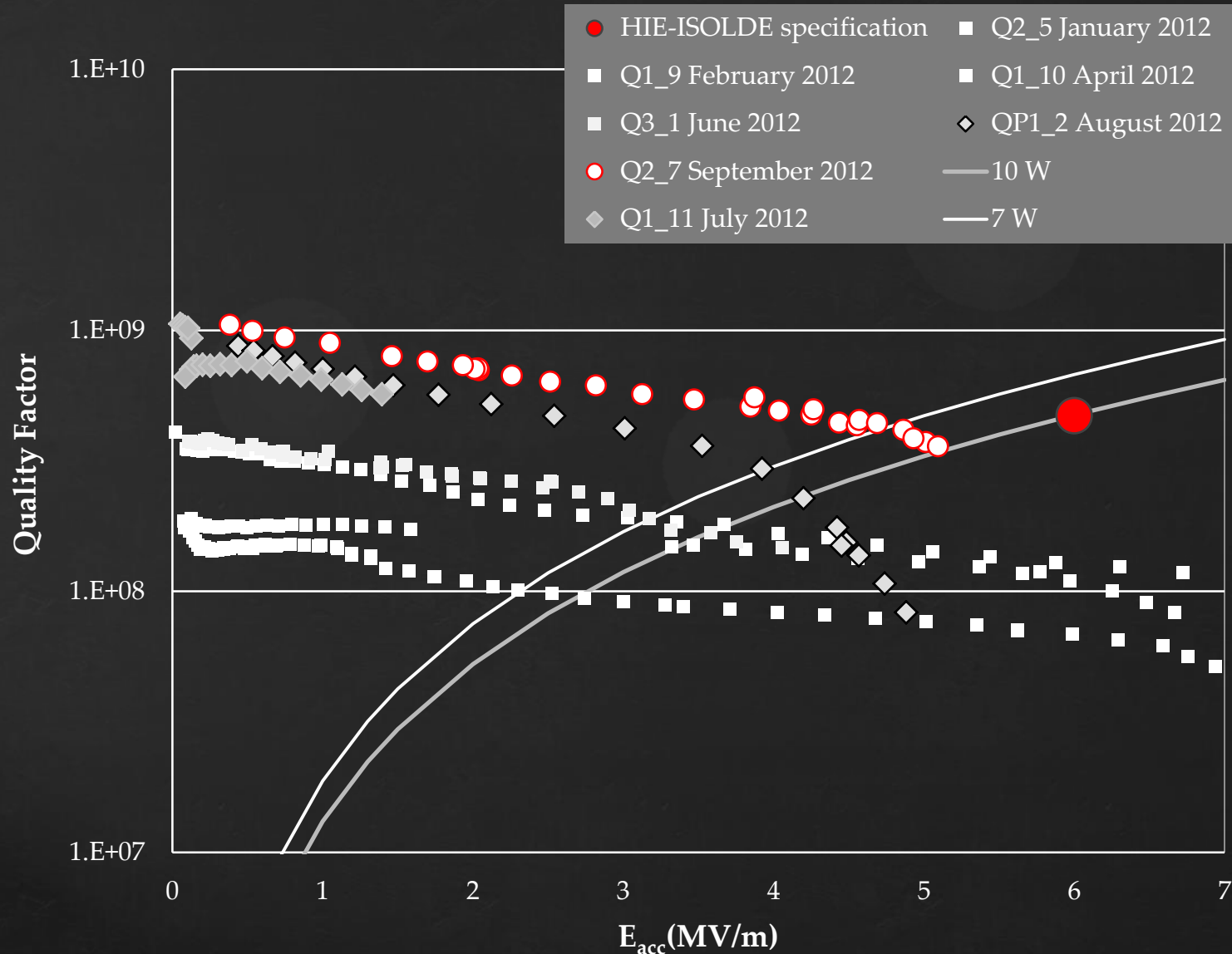
$$T_{(\text{bake out})} < T_{(\text{coating})} \rightarrow 600 \text{ }^\circ\text{C}$$



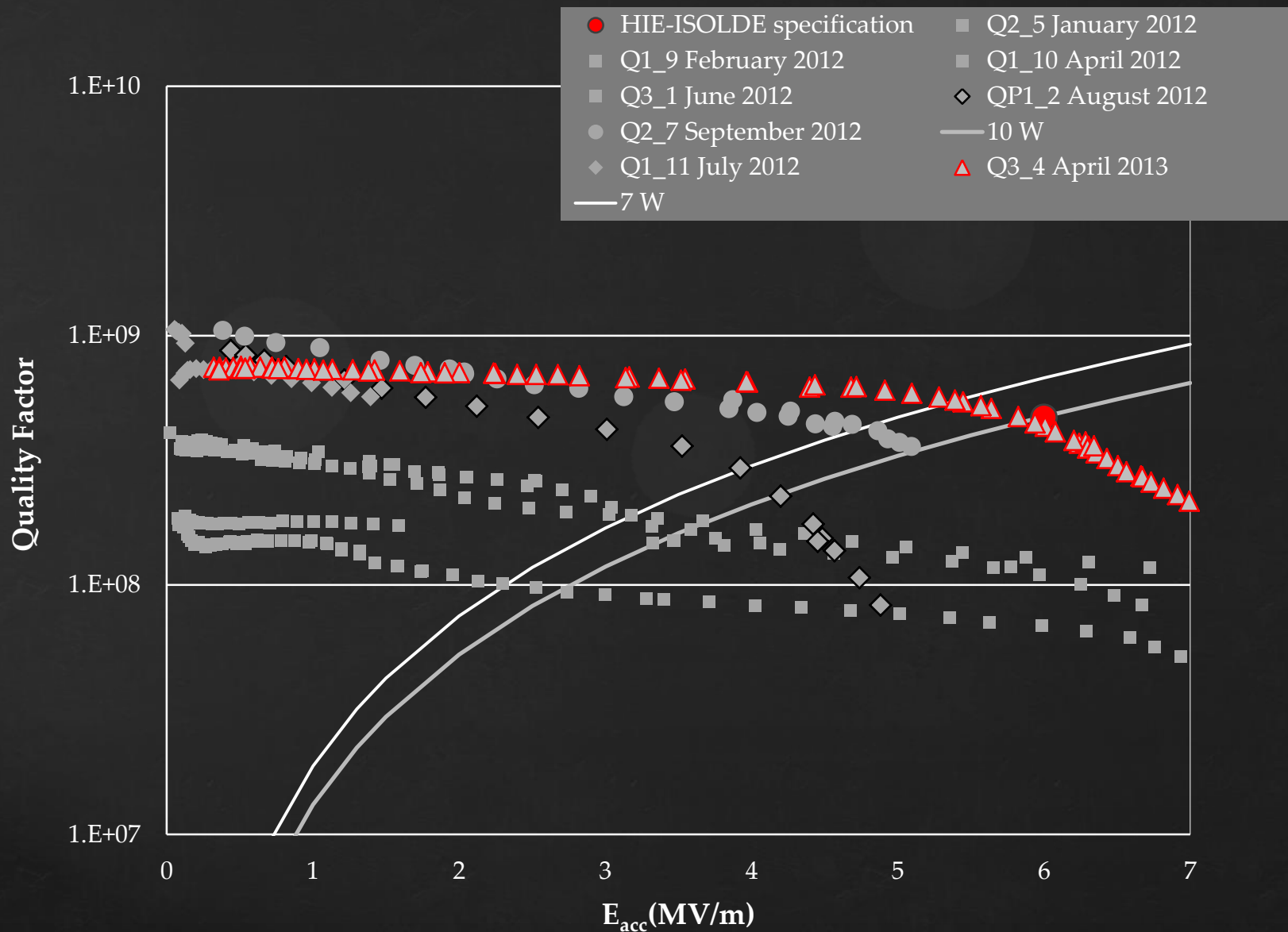
$T_{(\text{bake out})} > T_{(\text{coating})}$, higher sputtering power (layers),
change of gases: Kr, dry air \rightarrow Ar, N₂



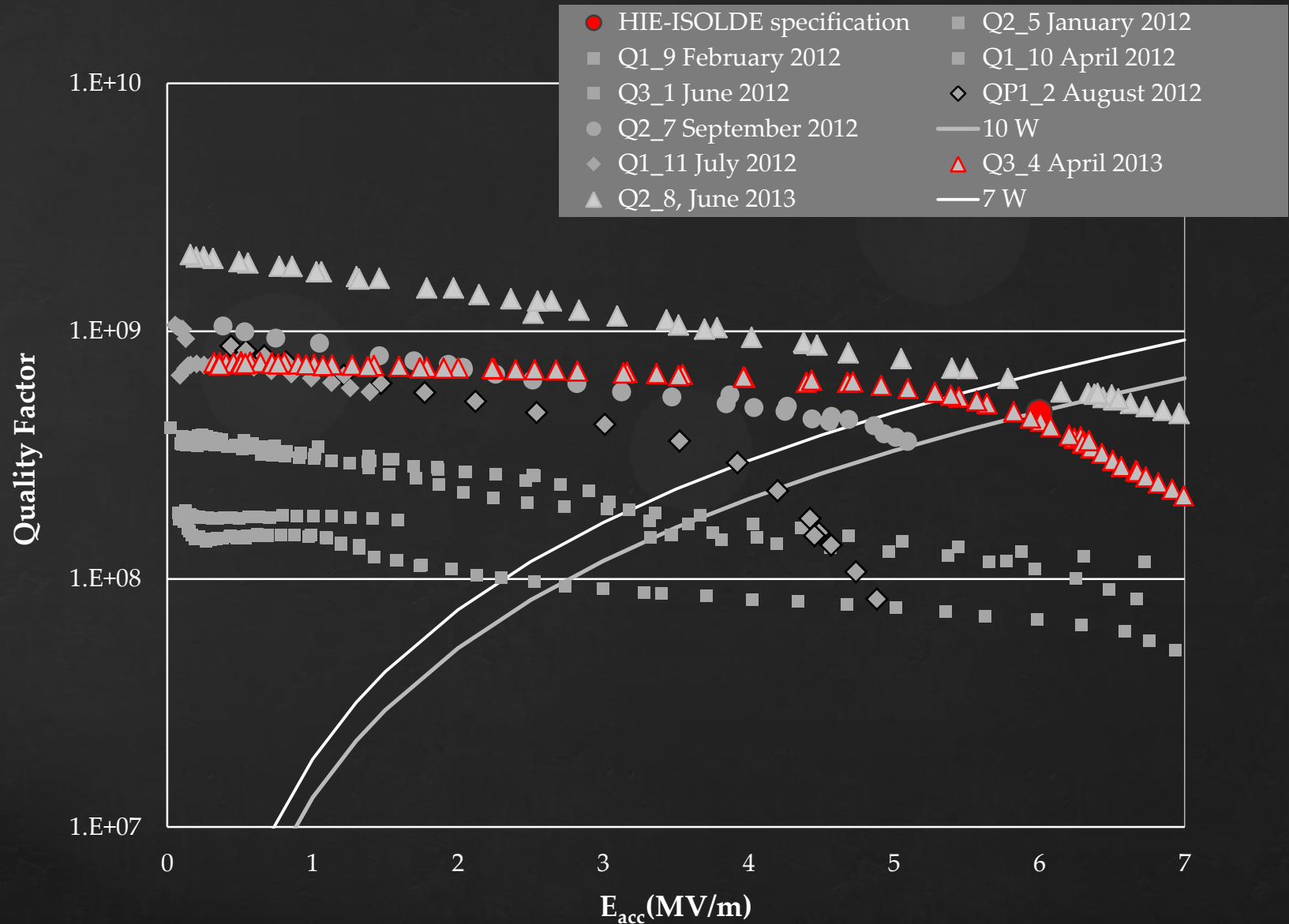
Increasing global Nb thickness by 25%



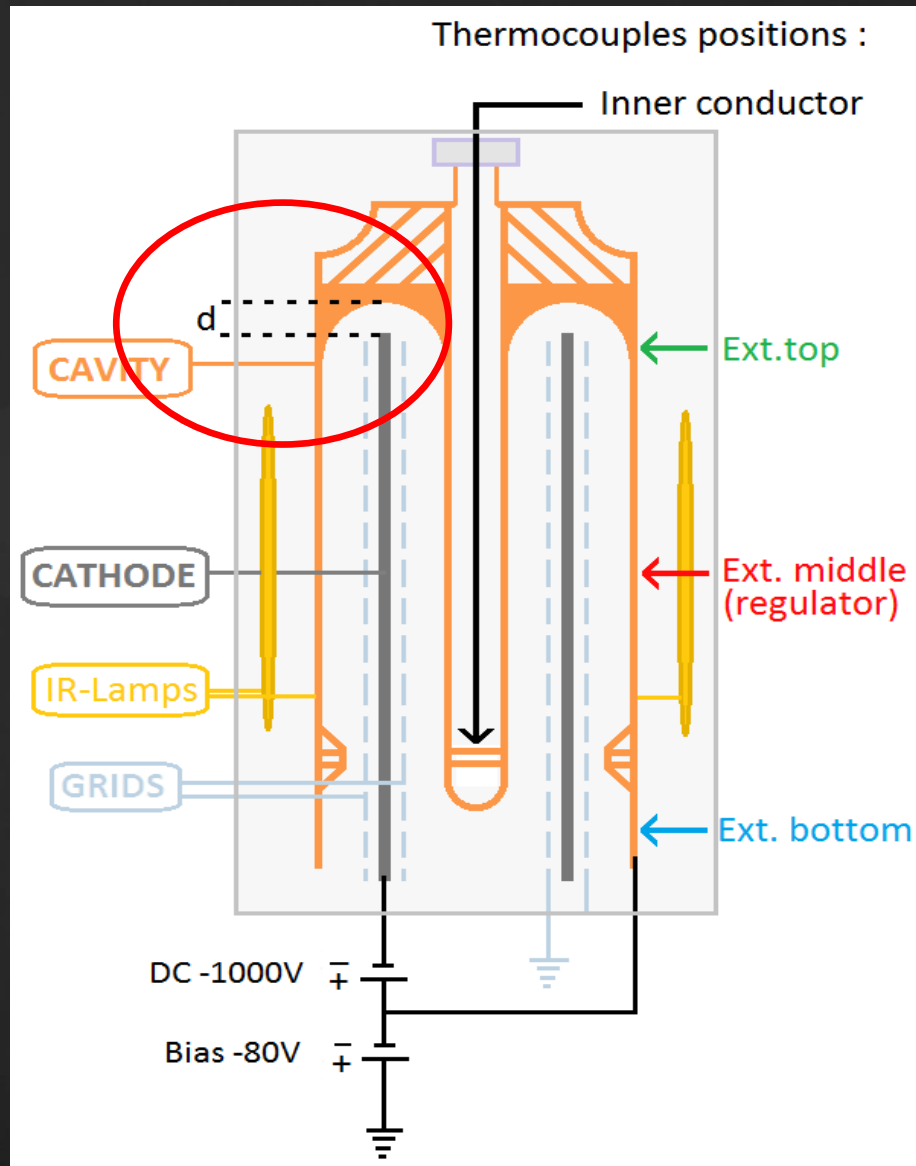
Reduced “top gap” length from 52 mm down to 32 mm



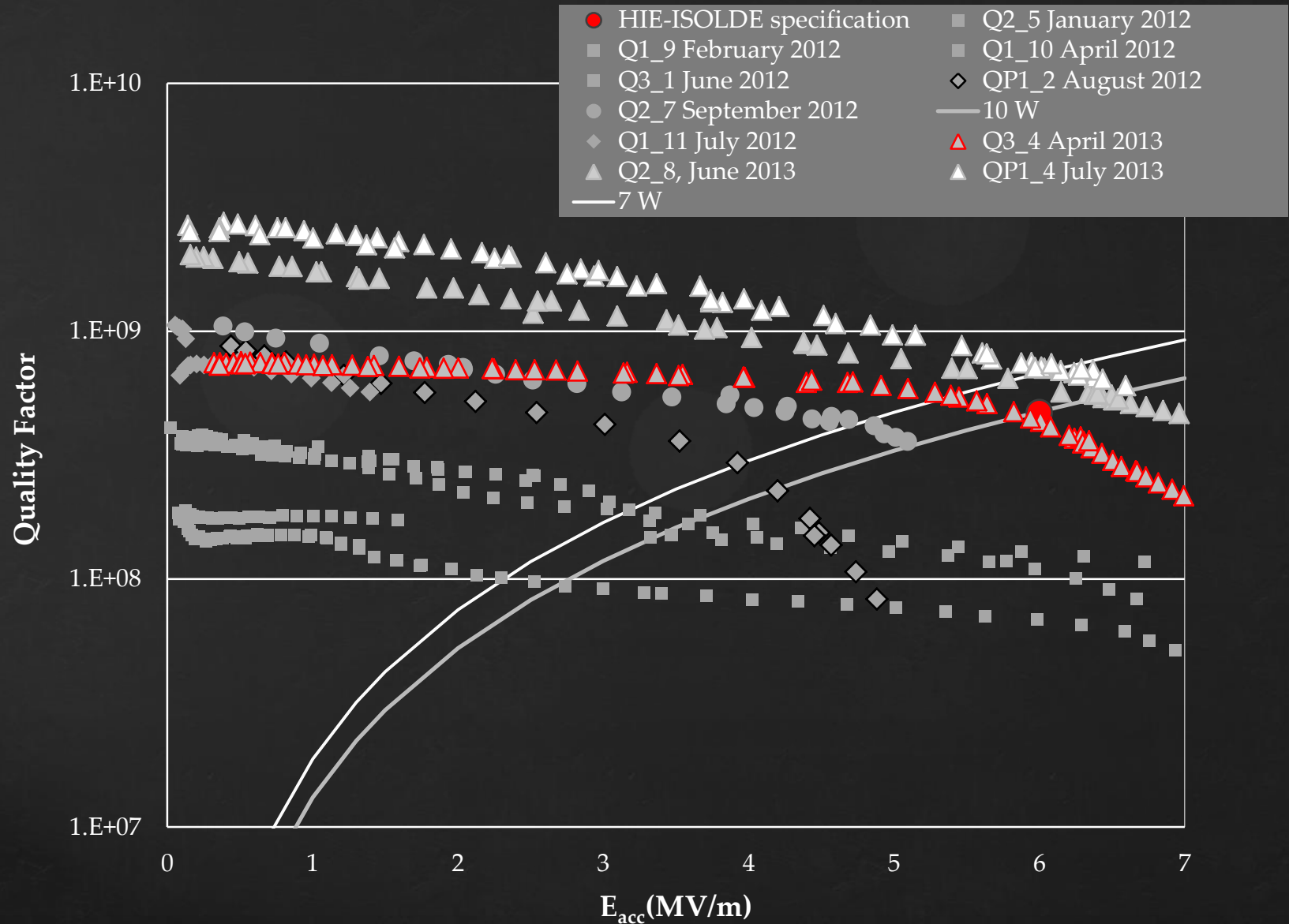
Same parameters on a 20 mm shorter substrate



Scaling the “top-gap” length

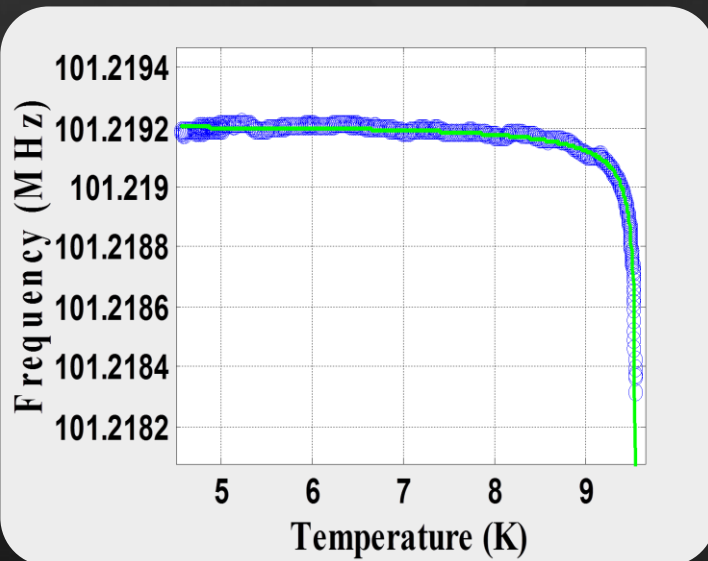


Top gap distance reduced to 22 mm



Average RRR extracted from $f_{\text{res}}(T)$ measurements

$\lambda_0 = 51 \pm 3$ nm
 $T_c = 9.55817 \pm 4e-5$ K
Freq = 101219201 ± 3.5 Hz
mfp = 64 ± 14 nm
 $\rho = (0.6 \pm 0.1) \mu\Omega \cdot \text{cm}$
RRR = 26 ± 5.5



Coating test	λ_0 (nm)	RRR
Q2_3 April 2011	188	1.9
Q1_5 June 2011	83	6.8
Q1_10 Feb. 2012	62.3	13.5
Q2_8 April 2013	50.7	26.4
Q3_4 March 2013	45.7	41.8

Surface quality of the inner conductor tip
→ field emission

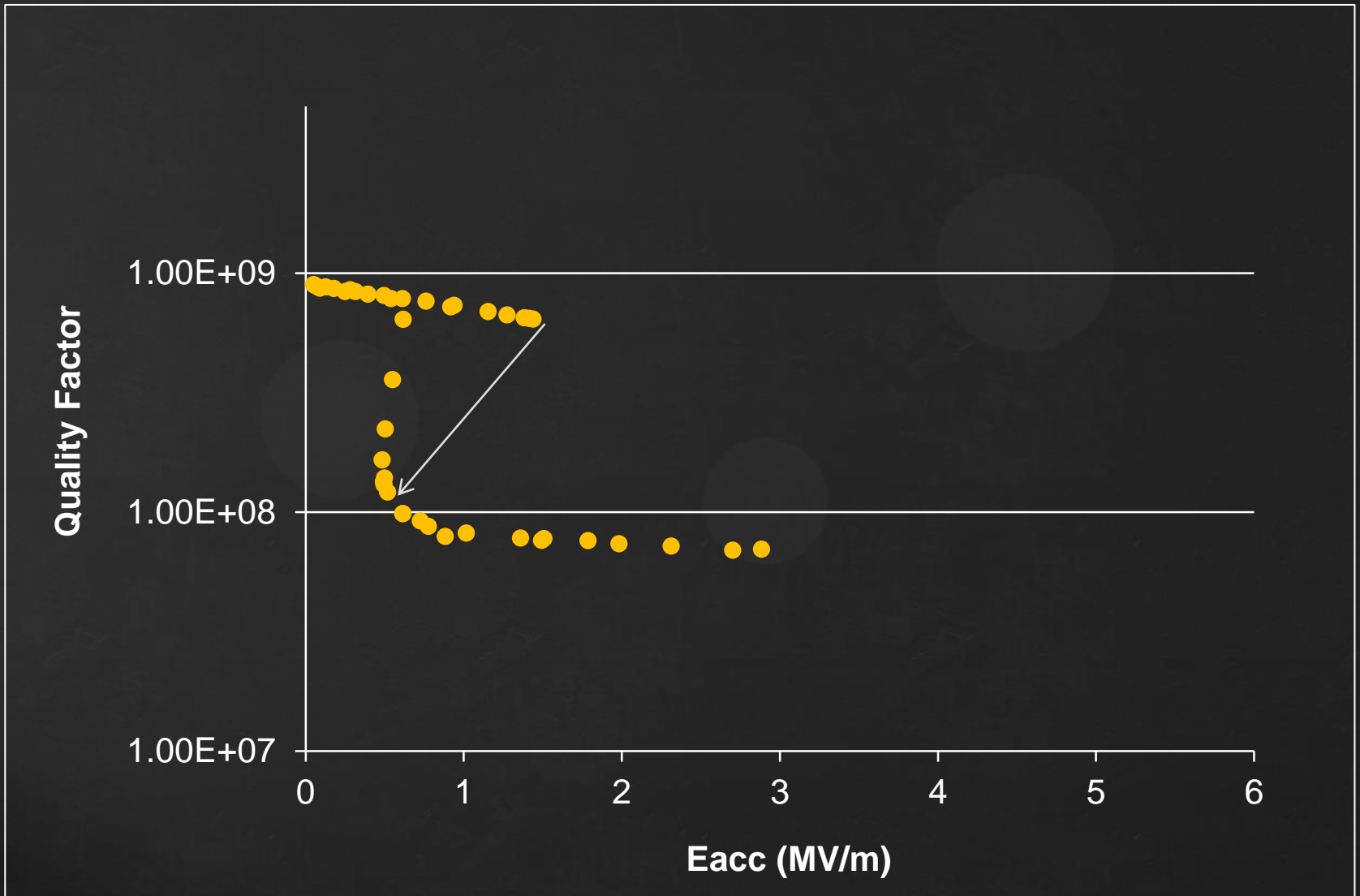


Central electrode: 20 mm
diameter, at earth potential



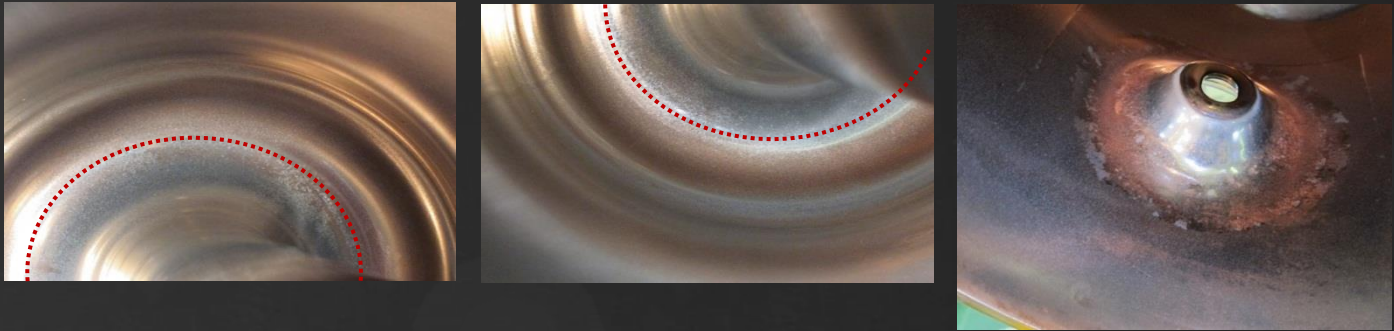
No counter electrode

Q switches



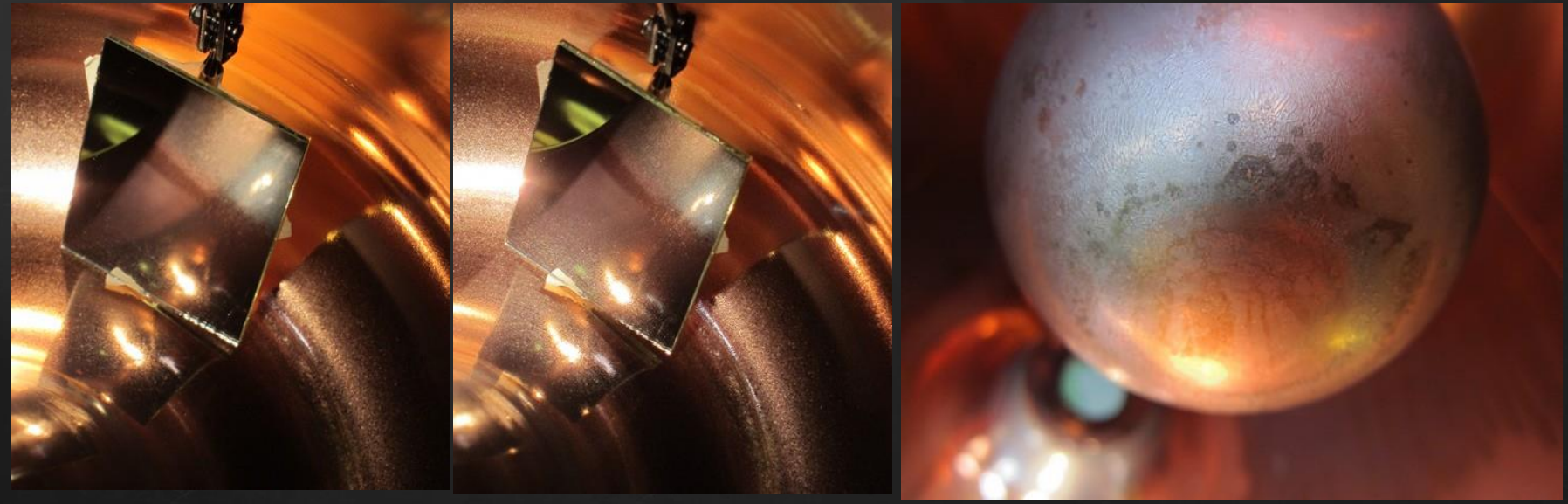
Investigating thickness/adhesion by step-stripping

Q1_11: Pictures after 15' stripping + 100bar rinsing
Cavity top (---- = welding ring)



Confirmed and integrated the information on thickness profile from beta-scope and sample measurements

Pictures after 15' +15' stripping + 100bar rinsing

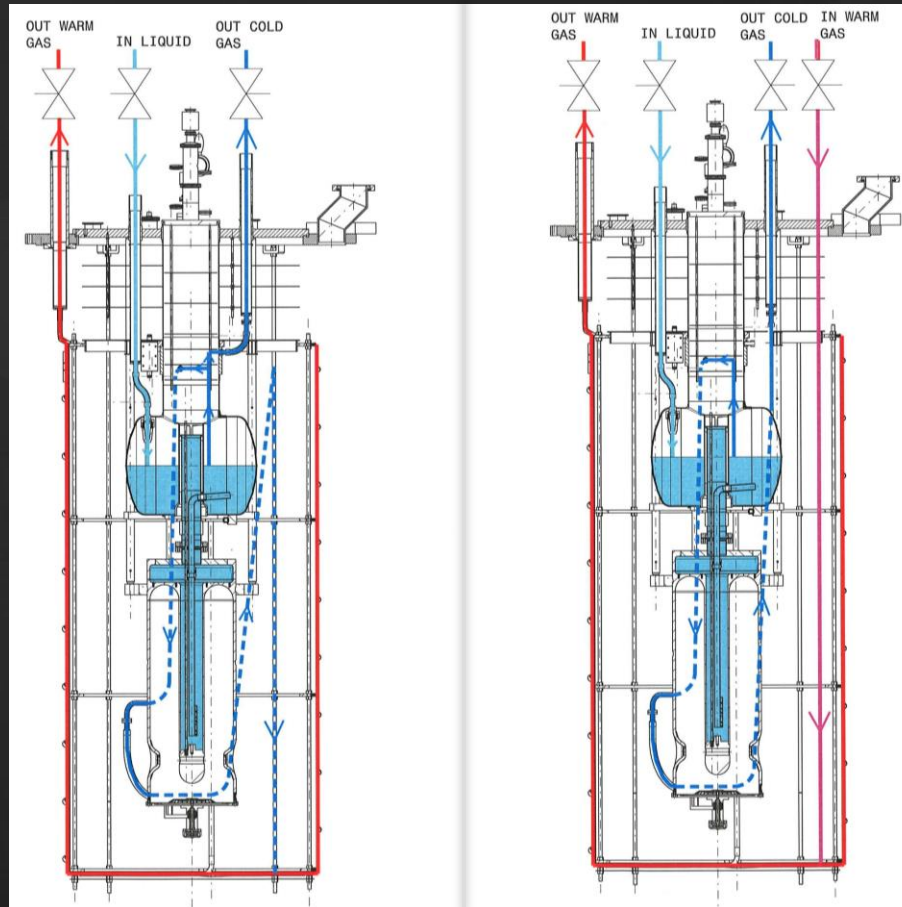


Cooling circuits: series vs. parallel

Phase I Test cryostat Phase II Test cryostat

Series:

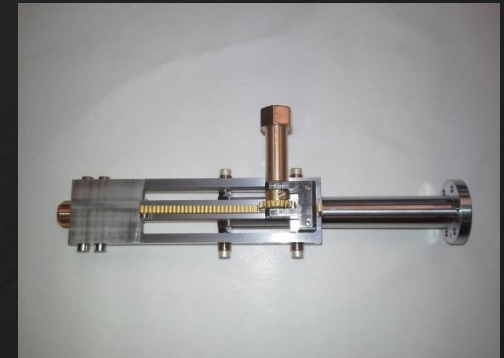
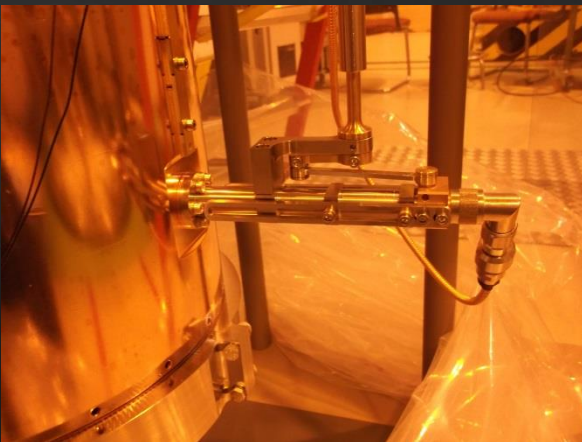
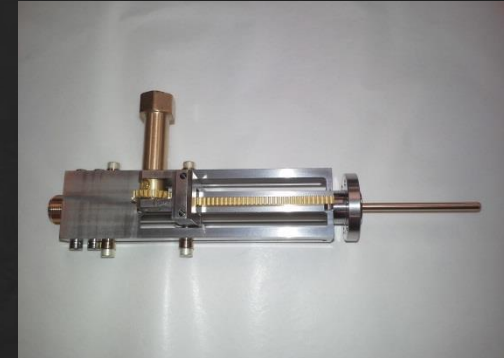
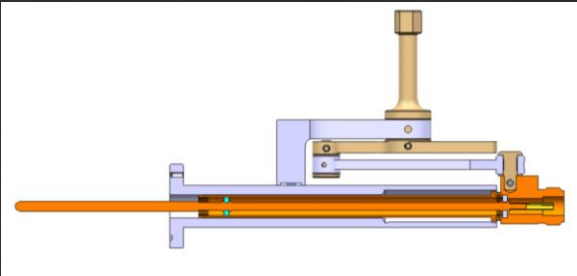
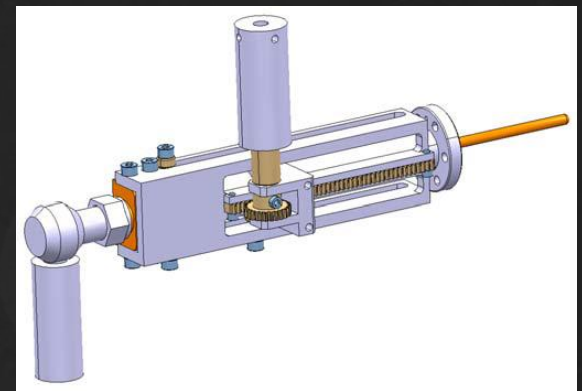
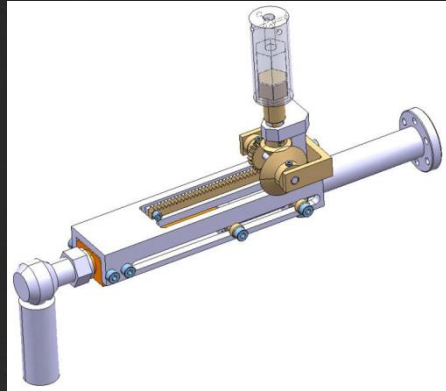
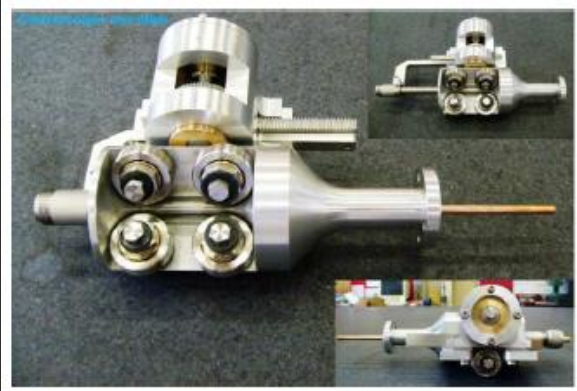
1. The He tank is cooled down
2. The cold gas is extracted and used to thermalize the RF cable
3. The gas is then directed to the thermal screen



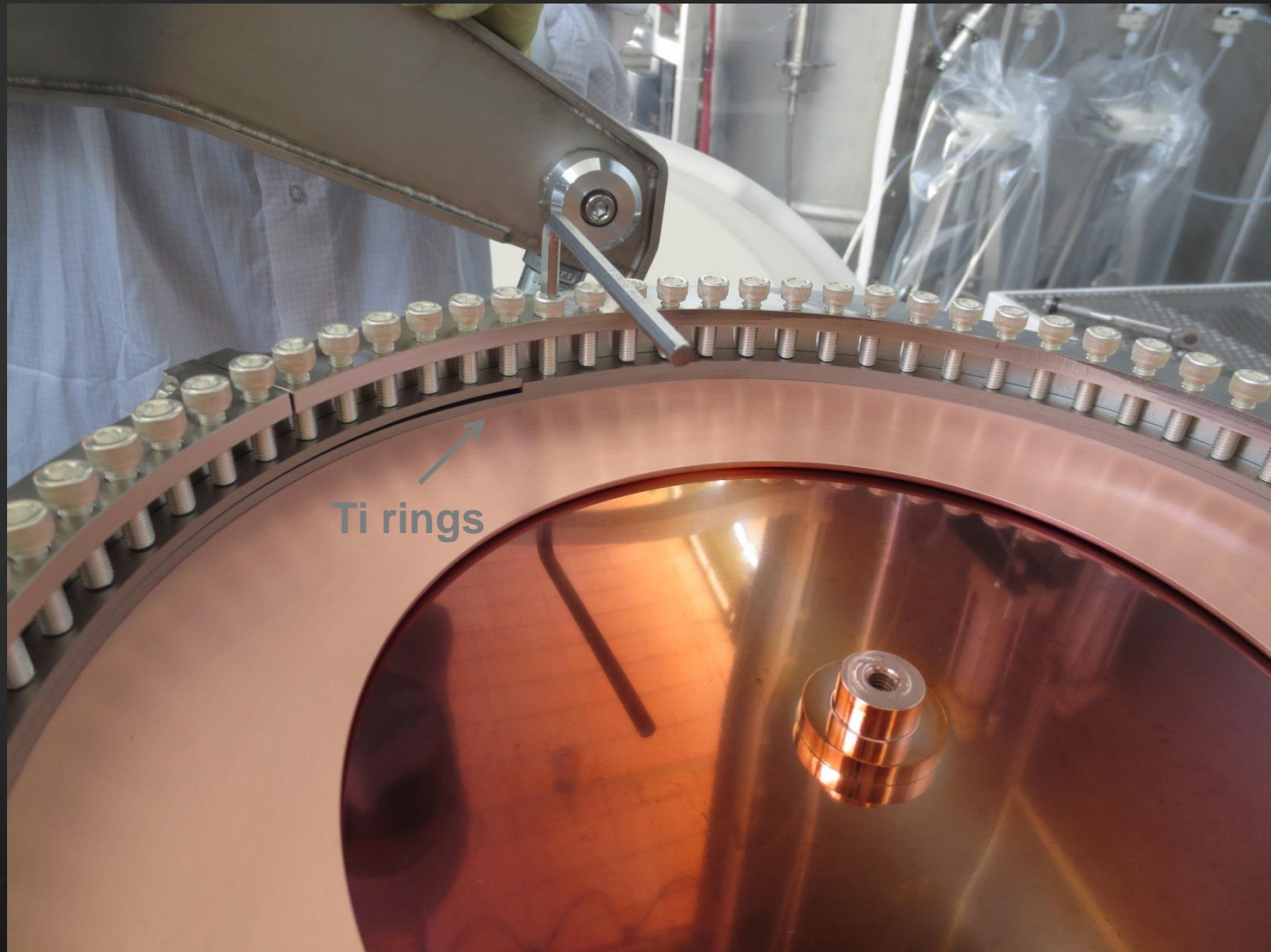
Parallel:

1. The He tank is cooled down
2. The cold gas is directed to thermalize the RF cable and extracted
3. An independent line feeds the thermal screen

Coupling system evolution



Tuning plate is fixed with 72 M6 screws closed at 5 Nm and acting on Ti rings



Pondering on the RF contact at cold...

GEOMETRIE

$$L_{cu} := 17\text{mm}$$

$$LL := 3\text{mm}$$

$$L_{ss} := L_{cu} + LL = 20\text{-mm}$$

BAGUE TITANE

$$J_{ti} := -L_{ss} \cdot \text{AISI304Integral} + L_{cu} \cdot \text{OFECuintegral} + LL \cdot \text{Ti6Al4VIntegral} = 1.086 \times 10^{-3}\text{-mm}$$

BAGUE INOX

$$J_{ss} := -L_{ss} \cdot \text{AISI304Integral} + L_{cu} \cdot \text{OFECuintegral} + LL \cdot \text{AISI304Integral} = 4.84 \times 10^{-3}\text{-mm}$$

CALCUL DE LA DEFORMATION ELASTIQUE (COMPRESSION) À CHAUD

$$\Delta L = \text{Faxial} \times \Sigma (l_0/EA)$$

$$\text{Abague} := \pi \left[\frac{(320\text{mm})^2 - (300\text{mm})^2}{4} \right] = 9.739 \times 10^3\text{-mm}^2$$

$$\text{VIS} = \text{M6 (72X)}$$

$$E_{cu} := 105 \cdot 10^3 \text{MPa} = 1.05 \times 10^{11} \text{Pa}$$

$$\text{Faxial} := 72 \cdot 6900 \text{N} = 4.968 \times 10^5 \text{N}$$

$$E_{ss} := 200 \cdot 10^3 \text{MPa} = 2 \times 10^{11} \text{Pa}$$

$$\text{Avis} := 72 \cdot 17.9 \text{mm}^2 = 1.289 \times 10^3\text{-mm}^2$$

$$E_{ti} := 110 \cdot 10^3 \text{MPa} = 1.1 \times 10^{11} \text{Pa}$$

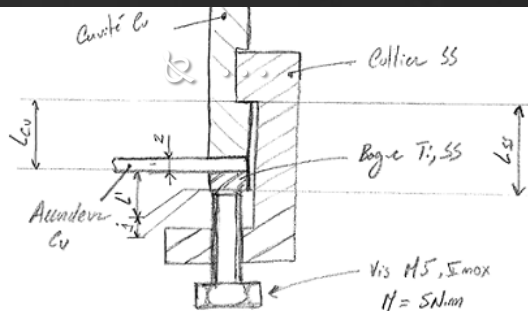
$$L_{vis} := 49\text{mm} - L_{ss} = 29\text{-mm}$$

BAGUE TITANE

$$\Delta L_{ti} := \text{Faxial} \cdot \left(\frac{L_{vis}}{E_{ss} \cdot \text{Avis}} + \frac{LL}{E_{ti} \cdot \text{Abague}} + \frac{L_{cu}}{E_{cu} \cdot \text{Abague}} \right) = 0.066\text{-mm}$$

BAGUE INOX

$$\Delta L_{ss} := \text{Faxial} \cdot \left(\frac{L_{vis}}{E_{ss} \cdot \text{Avis}} + \frac{LL}{E_{ss} \cdot \text{Abague}} + \frac{L_{cu}}{E_{cu} \cdot \text{Abague}} \right) = 0.065\text{-mm}$$



CALCUL DU RELACHEMENT À FROID

Les pertes de deformation (en compression) sont equivalentes aux pertes de serrage

$$\Delta L_{tifroid} := \Delta L_{ti} - J_{ti} = 0.064\text{-mm}$$

$$\frac{\Delta L_{tifroid}}{\Delta L_{ti}} = 98.343\%$$

% du serrage à chaud qui reste à froid

$$\Delta L_{ssfroid} := \Delta L_{ss} - J_{ss} = 0.06\text{-mm}$$

$$\frac{\Delta L_{ssfroid}}{\Delta L_{ss}} = 92.545\%$$

Si 2 bagues sont installées (LL=6mm):

$$\frac{\Delta L_{tifroid}}{\Delta L_{ti}} = 104.362\%$$

$$\frac{\Delta L_{ssfroid}}{\Delta L_{ss}} = 91.921\%$$

CONCLUSIONS:

Car la déformation par compression élastique des composants en série (~60um) soumis à la charge des vis est toujours plus importante que la contraction thermique (1-5um), le contact est toujours assuré, soit avec la bague en inox, soit avec la bague en titane.

Avec: -1 bague en titane (t=3mm), la pression de contact reste pratiquement la même (98%);

-2 bagues en titane (t=6mm), la pression de contact augmente de 4%;

-1 bague en inox (t=3mm), la pression de contact reste à 92% de la valeur initial;

-2 bagues en inox (t=6mm), la pression de contact reste aussi à env. 92%;

Remaining issue in 2014

Cavity Tuning

Available tuning range: 40 kHz

Statistics of warm to cold shift was known

Strategy to cut the cavity at reception

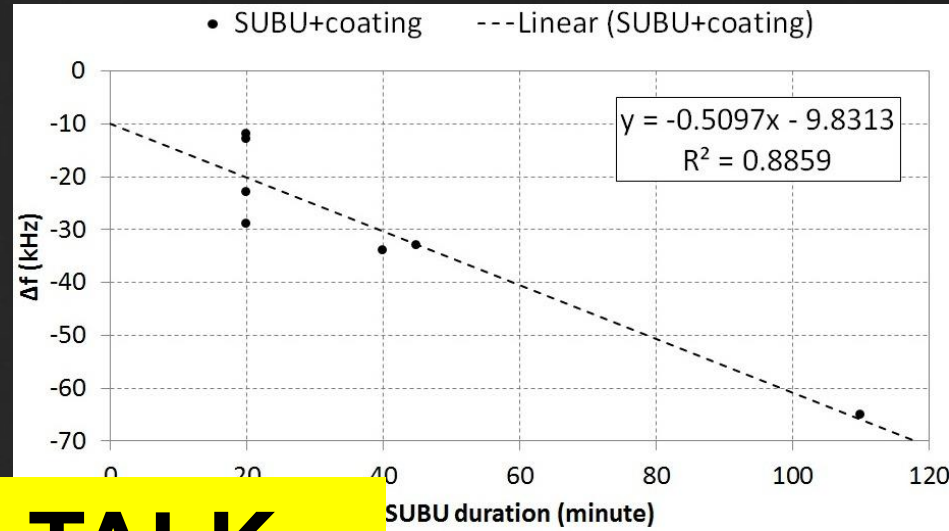
Something went wrong...

The first cavities had a higher-than-expected Δf !

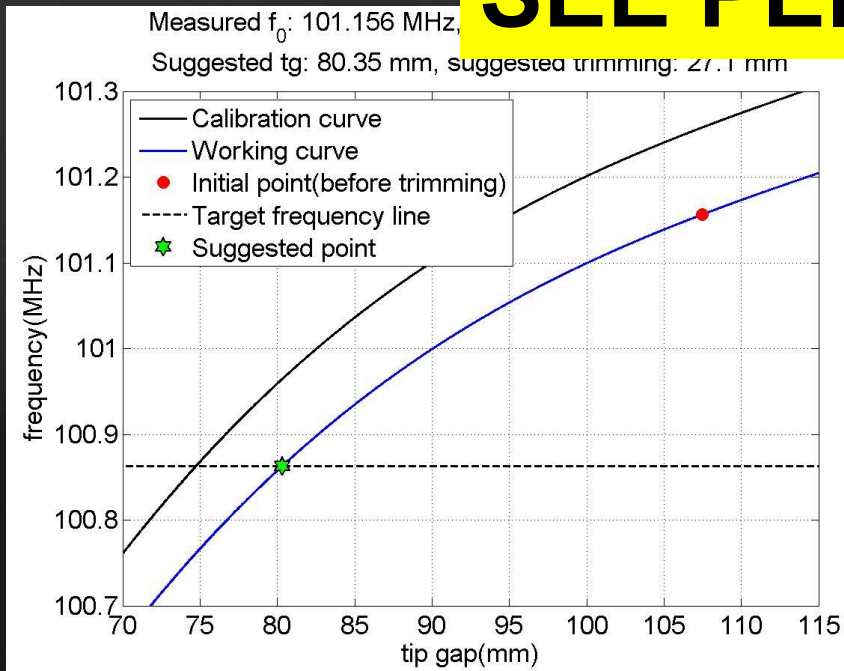
Investigations to find the reason took several months
(more in Pei's talk)

Cavity tuning, mystery solved

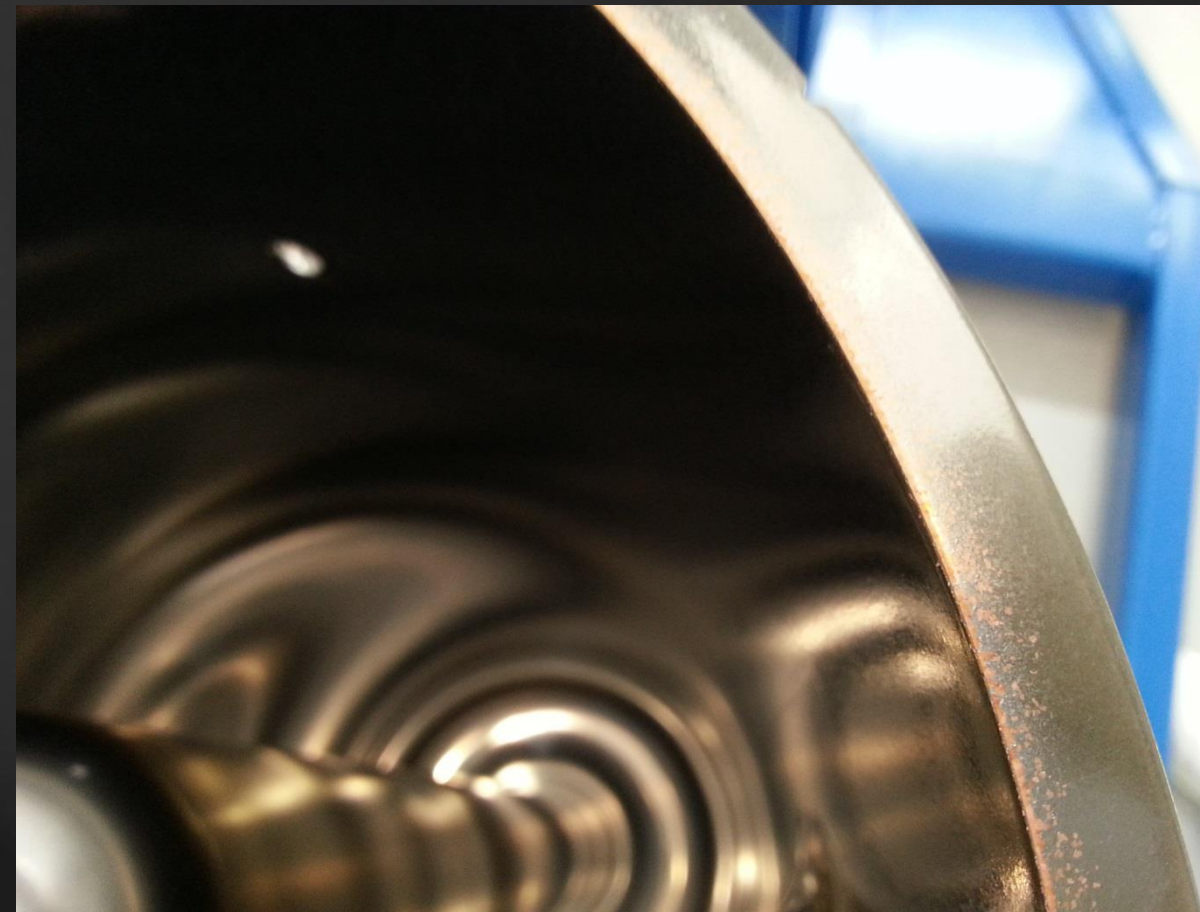
influence variables	frequency shift (kHz)
295 K to 4.5 K and air to vacuum	+371 +/- 5
chemical etching 40'	-27 +/- 3
Nb coating	



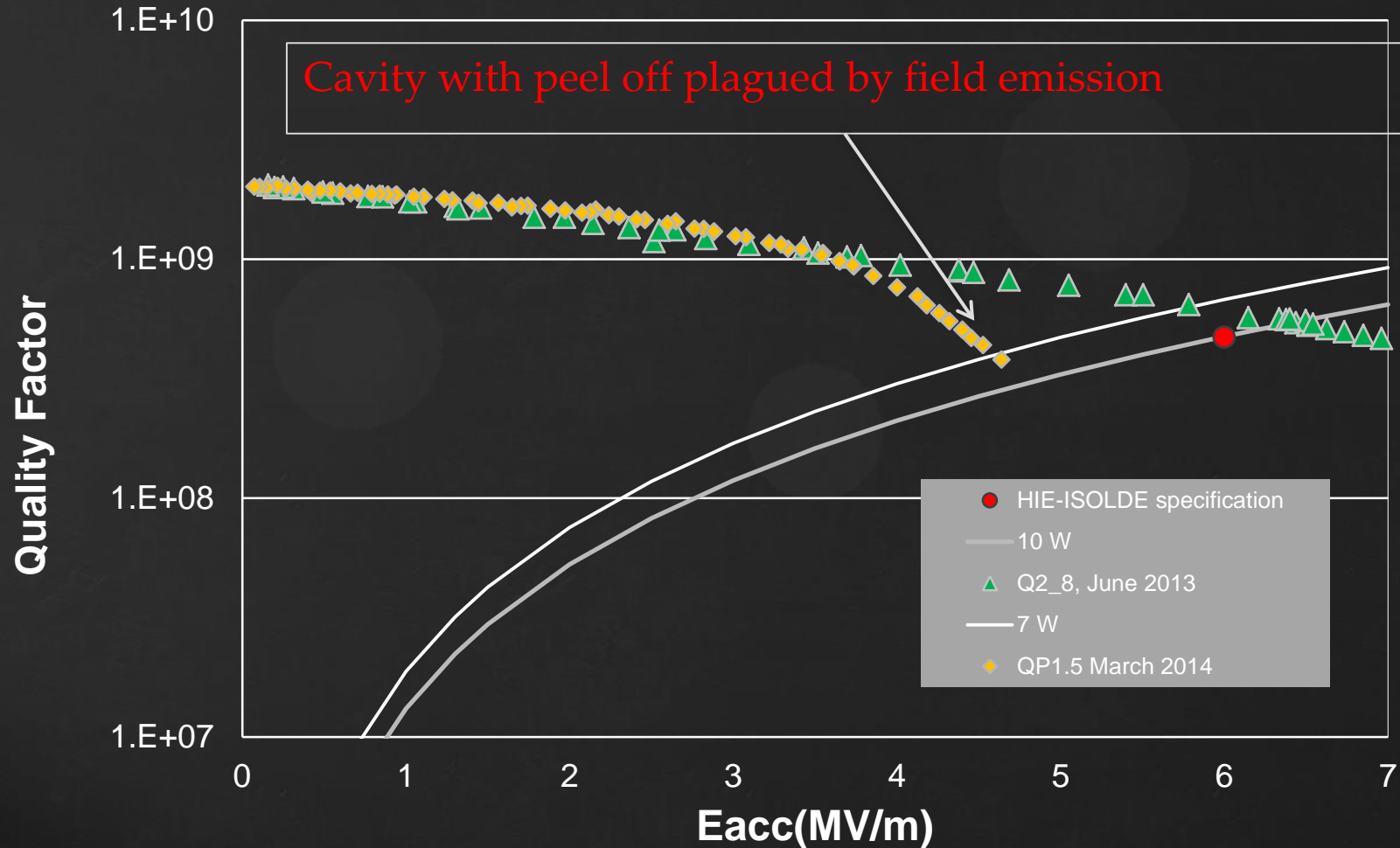
SEE PEI's TALK



Peel off of RF contact: the problem



Peel off of RF contact: the problem

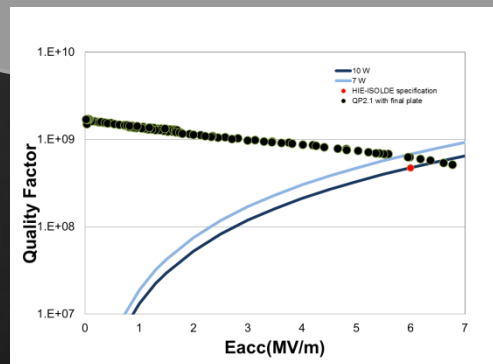
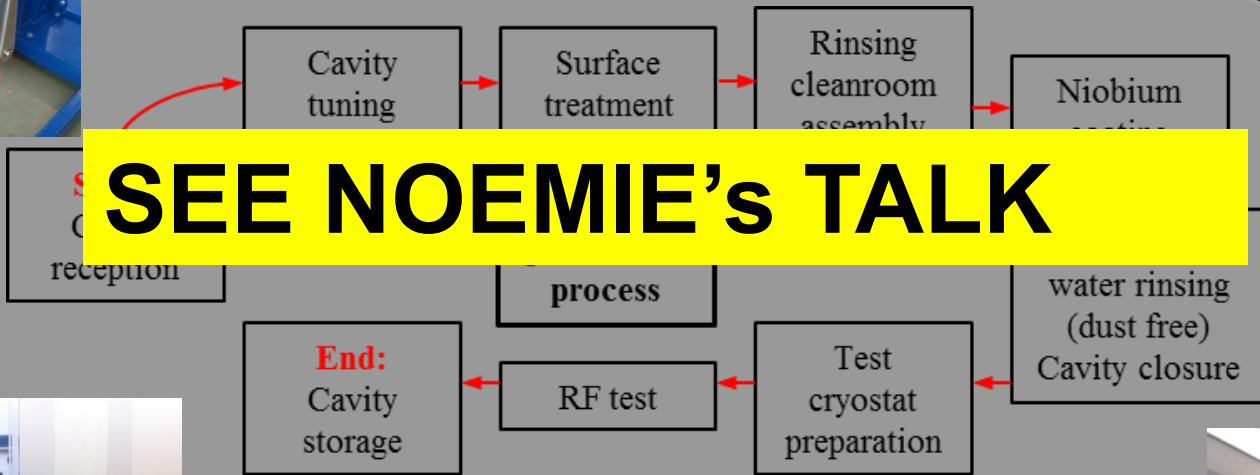
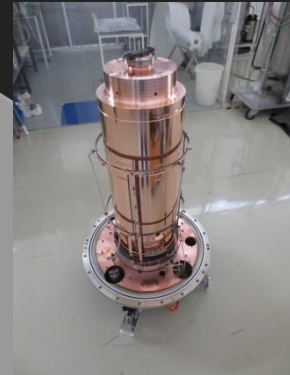
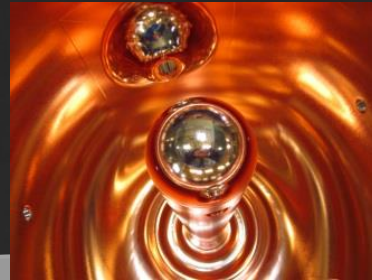


Peel off of RF contact: the solution





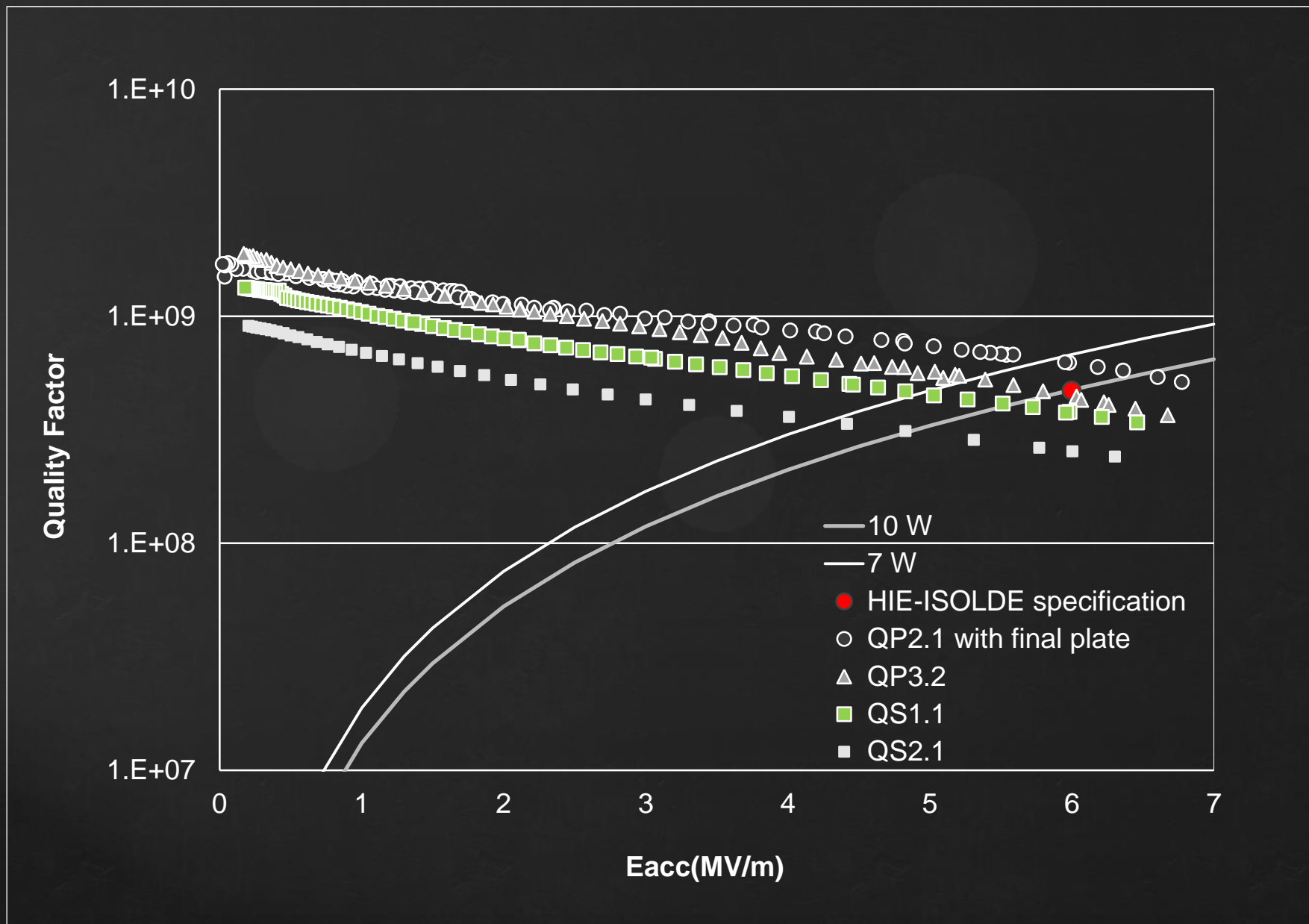
Cavity production workflow



Series substrates “teething” problems



Performance of the first 4 series cavities



RF systems (Power and LLRF)

- Low microphonics; sensitivity to He pressure
~ 0.01 Hz/mbar, no beam loading → high Q_L in operation
- → Eased design for the input coupler
- → 700 W solid state RF amplifiers
- State of the art digital LLRF system
 - Direct RF sampling
 - Digital quadrature demodulation
 - Direct RF generation by DAC
 - VME form factor, 1 LLRF controller card per cavity
- LLRF system installed in 14 shielded racks
- Reference RF phase distributed over the length of linac to allow automatic cavity phasing for different species

LLRF controller for one cavity



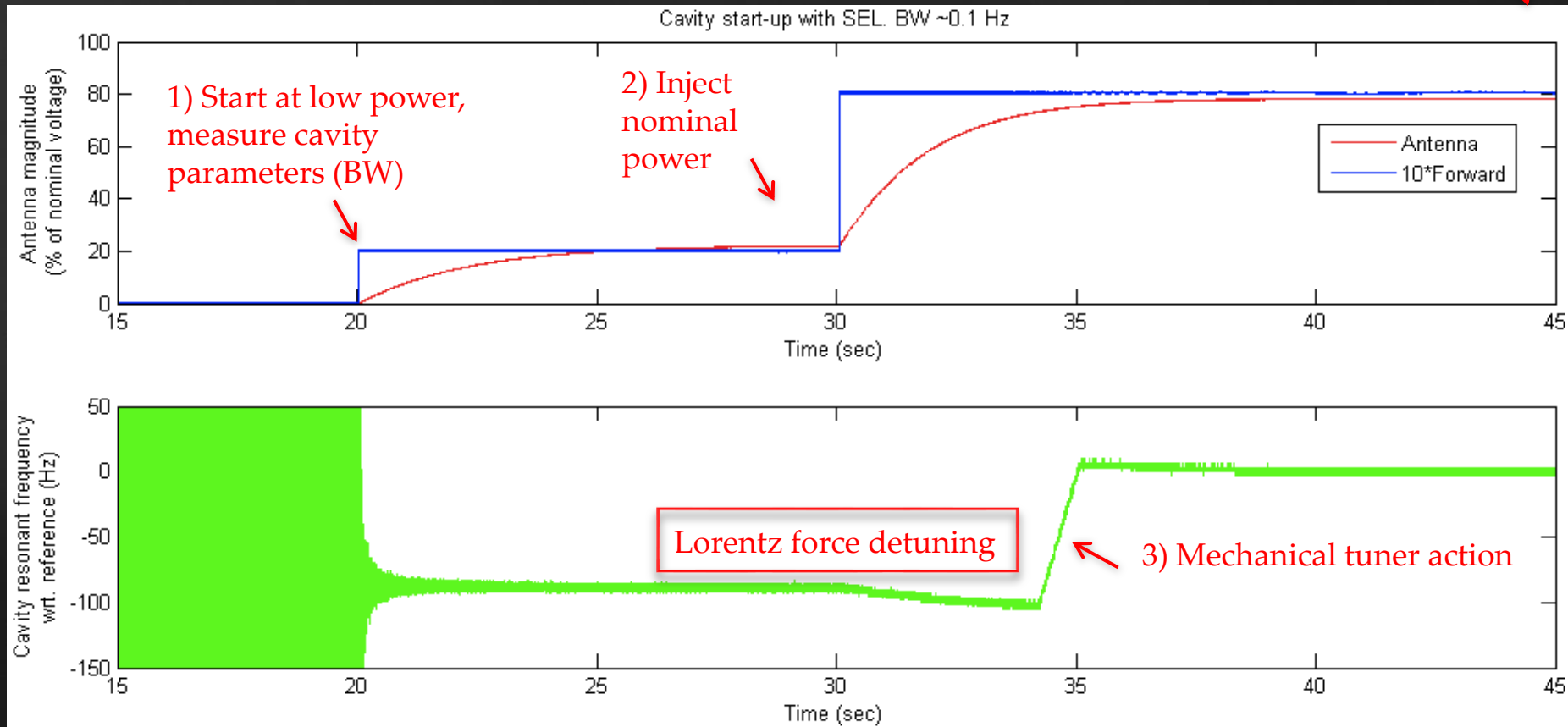
LLRF system for a complete cryomodule (6 cavities)



Low-Level RF system

- Example of a cavity start up with self excited loop

4) Switch over to generator driven mode, lock the loops



Conclusion

The HIE-ISOLDE working group on accelerating structures was the crucible of all the developments which made possible to achieve the specified performance of the HIE ISOLDE superconducting cavities.

The CATHI fellows played a key role: thank you!

Much work and unknowns are still in front of us towards the final goal of delivery the first beams from HIE-ISOLDE to the experiments, but all the ingredients are now in our hands thanks to the work of these years

Acknowledgments

M. Pasini, one of the initiators of the HIE ISOLDE project and first ASWG chairman

The technical staff at CERN

G. Bisoffi, E. Palmieri, S. Stark, A. Porcellato from INFN-LNL

The HIE ISOLDE teams at CERN

Belgian Big Science program of the FWO (Research Foundation Flanders)

and the Research Council K.U. Leuven.

CATHI Marie Curie Initial Training Network: EU-FP7-PEOPLE-2010-ITN Project number 264330.

The HIE ISOLDE International Advisory Panel

The CERN management

References

- [1] H. Padamsee, J. Knobloch, T. Hays “RF Superconductivity for accelerators” Wiley-VCH
- [2] A. Facco “Tutorial on low beta cavity design” proceedings of SRF 2005
- [3] C. Benvenuti, N. Circelli and M. Hauer, “Niobium films for superconducting accelerating cavities”, Appl. Phys. Lett., Vol. 45. No.5, September 1984.
- [3] C. Benvenuti *et al*, “Superconducting Niobium Sputter-coated Copper Cavity Modules for the LEP Energy Upgrade”, Proceedings of the Particle Accelerators Conference, PAC1991, vol. 2, pp. 1023-1025
- [4] M. Pasini, *et al*, “A SC upgrade for the REX-ISOLDE accelerator at CERN,” Proceedings of LINAC08, 2008, Victoria, BC, Canada.
- [5] V. Palmieri, V. L. Ruzinov, S. Stark, *et al*, “New Results on Niobium sputtered Copper quarter wave resonators” Proc. of the Sixth Workshop on RF Superconductivity, Newport News, Virginia, 1993
- [6] A. M. Porcellato *et al*, “Performance of ALPI new medium beta resonators” Proceedings of HIAT 2012, Chicago, IL, USA; and references therein
- [7] G. Lanza, *et al*, “The HIE ISOLDE Superconducting cavities: surface treatment and Niobium thin film coating” Proceedings of SRF09, p. 801
- [8] A. D’Elia, R. M. Jones, and M. Pasini, “HIE-ISOLDE high beta cavity study and measurement” Proceedings of SRF09, p. 609
- [9] L. Alberty *et al*, “The copper substrate developments for the HIE-ISOLDE high-beta QWRs”, these proceedings
- [10] N. Jecklin *et al*, “Niobium Coatings for the HIE ISOLDE QWR superconducting accelerating cavities”, proceedings of SRF13.
- [11] W. Venturini Delsolaro *et al*, “Status of the superconducting RF activities for the HIE_ISOLDE Project”, Proceedings of LINAC12, Tel-Aviv, Israel, September 2012.
- [12] A. Sublet *et al*, “Preliminary Results of Nb Thin Film Coating for HIE-ISOLDE SRF Cavities Obtained by Magnetron Sputtering”, these proceedings
- [13] S. Stark *et al*, “Nb sputter-coated QWRs” Particle Accelerators, Vol. 61 (1998), p. 383
- [14] J.A. Thornton, J. Vac. Sci. Technol., 11 (1974), p. 666
- [15] C. Benvenuti *et al*, “Study of the Surface Resistance of Niobium Sputter-Coated Copper Cavities” IEEE Transactions on Applied Superconductivity, Vol. 9, No. 2, p. 900, June 1999
- [16] A. M. Sublet *et al*, “Thin Film Coating Optimization for HIE-ISOLDE SRF Cavities: Coating Parameters Study and Film Characterization ” these proceedings
- [17] J. Popielarski *et al*” Dewar testing of beta=0.085 Quarter Wave Resonators at MSU”, Proceedings of SRF2011, Chicago, IL, USA, p. 539
- [18] P. Zhang *et al*, “The tuning system for the HIE ISOLDE high beta Quarter Wave Resonator” these proceedings
- [19] C.J. Gorter and H.B.G. Casimir, Z. Tech. Phys., **15**, 539, 1934
- [20] A. D’Elia, “A method to evaluate RRR of superconducting cavities’ CERN-HIE-ISOLDE-PROJECT-Note-0014, September 2012